Fluid Phase Equilibria 587 (2025) 114212

Contents lists available at ScienceDirect

Fluid Phase Equilibria

journal homepage: www.journals.elsevier.com/fluid-phase-equilibria

Preferential solvation in pharmaceutical processing: Rigorous results, critical observations, and the unraveling of some significant modeling pitfalls

Ariel A. Chialvo

Knoxville, TN 37922-3108, USA

ARTICLE INFO

Keywords:
Universal preferential solvation function
Preferential interaction parameters
Fundamental structure making/breaking functions
Kirkwood-buff inversion
Thermodynamic pitfalls
Pharmaceutical species
dilute ternary systems

ABSTRACT

We probe the solvent effects on the preferential solvation of pharmaceutical species in mixed-solvent environments, identify its universal molecular-based signature, and characterize explicitly the macroscopic-to-microscopic formal connections between the thermodynamic non-idealities and the precisely defined *fundamental structure making/breaking functions* $\mathscr{I}_{\alpha\beta}(T,P,x_\alpha)$. For that purpose, we link the thermodynamic response of the solute triggered by changes in the mixed-solvent environment to either a linear combination of $\mathscr{I}_{\alpha\beta}(T,P,x_\alpha)$ or *the universal preferential solvation function* $\mathscr{PI}(T,P,x_\alpha)$. Then, we illustrate the proposed approach by analyzing the solvation behavior of a series of pharmaceutical solutes in both aqueous-organic and mixed-organic environments at ambient state conditions. Moreover, we briefly discuss the tenets of a popular local composition-based model of preferential solvation, present a forensic analysis of the Kirkwood-Buff inversion expressions invoked in its implementation, and identify some pervasive modeling pitfalls as well as their associated common causes and concomitant consequences. Finally, we highlight the significance behind the analysis of preferential solvation phenomena, provide some pertinent observations on the findings, and offer a consistent outlook.

1. Introduction

Chemical processes are typically conducted in condensed fluid phases involving both neat and mixed-solvents, where the choice of appropriate solvents (or mixed-solvents for that matter) depends on many factors including the nature of the solutes and the type of process under consideration [1–3]. Mixed-solvents are often more convenient solvation environments than neat solvents, in that, mixed-solvents allow the tuning of the desired properties such as their solvation power resulting from synergistic effects which are composition as well as pressure and temperature dependent [4–8]. In turn, the ability to tailor the solvation behavior of species lends the opportunity to manipulate the kinetic rate constants of reactions in solution resulting from the differential solvation of the reactants, transition state species, and reaction products, according to their intermolecular interaction asymmetries [9–14]

Synergistic cosolvent-induced enhancement of solubility involves the solvation phenomenon of common occurrence and practical relevance in processing technologies involving non-polar compressed gases and polar solvents such as in gas-expanded liquids [15–17] and entrainer-modified supercritical fluids [18–20]. On the one hand, cosolvents can increase significantly the solubility of non-polar drugs over that in aqueous environments, making viable the effective formulations of concentrated solutions of non-polar drugs for systemic therapeutic treatments [21,22]. On the other hand, co-non-solvency — the unusual solvation phenomenon underlying the drastic reduction of solubility of a given solute in mixed-solvent environments whose individual components exhibit good solvency — might become a versatile tool to manipulate solute aggregation and/or crystallization toward specific pharmaceutical applications [23–25]

However, while often overlooked, the rational manipulation of the species solvation requires a fundamental molecular-based understanding of the solute-induced microstructural perturbation of the mixed-solvent environment (local inhomogeneities plus ensuing propagation) and their associated thermodynamic responses [26]. In search for that understanding, we must first recognize the relative affinity of the solute within its mixed-solvent environment as the common feature among these systems, which becomes the key for any attempt to rationally control the solvation behavior of any solute. Since the contrasting affinity manifests as a differential perturbation of the solvent environment relative to that of the cosolvent around the solute, it also reveals as distinctive microstructural signatures which can be rigorously linked to experimentally available thermodynamic properties [5,27–30]. In fact,

E-mail address: ovlaich@gmail.com.

https://doi.org/10.1016/j.fluid.2024.114212
Received 4 July 2024; Received in revised form 1 August 2024; Accepted 21 August 2024
Available online 22 August 2024

Nomenclature

Symbols

$B_{\alpha}^{*,\rho}(T,P)$ second osmotic virial coefficient of the α − species
DCFI direct correlation function integral
$\mathscr{D}(T,P,x_j)$ diffusive or material stability coefficient $\left[1+\left(\partial \ln\gamma_j/\partial \ln x_j\right)_{TP}\right]$
$f_{\alpha}(T,P,x_{\alpha})$ fugacity of the $\alpha-$ species
$g_{i\alpha}(r_{i\alpha})$ radial distribution function for the $i\alpha-$ centers of mass interactions
$h_{i\alpha}(r_{i\alpha})$ pair correlation function for the $i\alpha-$ centers of mass interactions, i.e., $h_{i\alpha}(r_{i\alpha})=g_{i\alpha}(r_{i\alpha})-1$
$g^{E}(T,P,x_{\alpha})$ isobaric-isothermal excess Gibbs free energy of the binary mixed-solvent
$G_{\alpha\beta}(T,P,x_{\alpha})$ Kirkwood-Buff integral for the $\alpha\beta-$ interactions
$\mathscr{H}_{i,j}^{IS}(T,P)$ Henry's law constant of an $i-$ species in a j − solvent given by $\mathscr{H}_{i,j}^{IS}(TP)=f_i^{o}(TP)\gamma_i^{LR,\infty}(TP)$
k Boltzmann constant
KB Kirkwood-Buff
$\mathscr{N}_{i\alpha}\left(R_c^{i\alpha}\right)$ represents the average number of $\alpha-$ solvent within the correlation shell of radii $R_c^{i\alpha}$
$\mathscr{PS}(T,P,x_{\alpha})$ universal preferential solvation function
$\mathscr{P}^{E}(T,P,x_{\alpha})$ generic isobaric-isothermal excess property of the mixed-solvent
$R_c^{i\alpha},R_c$ radius of the correlation volume where the local composition is defined
$\mathscr{S}_{\alpha\beta}(T,P,x_{\alpha})$ structure making/breaking function for the $\alpha\beta$ − interactions
TCFI otal correlation function integral, *aka* total correlation function integral, *aka* Kirkwood-Buff integral
T,P state conditions defined by the system temperature and pressure
T,ρ_o state conditions defined by the system temperature and density
$V_c^{i\alpha},V_c$ correlation volume where the local composition is defined
$\widehat{v}_{\alpha}(T,P,x_{\alpha})$ partial molecular/molar volume of the α − species
x_{α} liquid phase composition defined by the mole fraction of the $\alpha-$ species
$x_{\alpha i}^{L}$ local mole fraction of $\alpha-$ species around the i − species
z_{α}^{o} compressibility factor $P/\rho kT$ for the pure α − species
β $(kT)^{-1}$
χ_{α} generic composition scale for the $\alpha-$ species, e.g., $\chi_{\alpha}\equiv(\rho_{\alpha},m_{\alpha},x_{\alpha})$
$\delta_{\alpha i}(R_c,x_{\alpha})$ deviation of the local mole fraction of the α − solvent around the $i-$ solute, *aka* preferential solvation parameter
$\delta_{\alpha i}^{0}$ Ben-Naim's first-order preferential solvation parameter
$\Delta_{\alpha\beta}(T,P,x_{\alpha})$ linear combination of Kirkwood-Buff integrals as marker of deviations from Lewis-Randall ideality, i.e., $\left(G_{\alpha\alpha}+G_{\beta\beta}-2G_{\alpha\beta}\right)_{TP}$
$\Delta_{tr}g_i(T,P,x_j)$ transfer Gibbs free energy of the $i-$ solute
$\Delta_{tr}\widehat{v}_i^{\ominus}(T,P,x_j)$ standard partial molar/molecular volume of transfer of the $i-$ solute
$\ln\widehat{\phi}_{\alpha}(T,P,x_{\alpha})$ partial molecular/molar fugacity coefficient of the $\alpha-$ species
$\ln(\widehat{\phi}_i z)^{\infty}$ $(kT)^{-1}-$ times the isochoric-isothermal residual chemical potential of the $i-$ solute at infinite dilution in the mixed-solvent environment
$\lambda_{\alpha}(T,\rho_{\alpha})$ absolute activity of the $\alpha-$ species
$\gamma_{\alpha}^{LR}(T,P,x_{\alpha})$ Lewis-Randall's activity coefficient of the $\alpha-$ species, *i.e.*, $\widehat{\phi}_{\alpha}(T,P,x_{\alpha})/\phi_{\alpha}^{o}(T,P)$
$\Gamma_{ij}^{(x_i\to 0)}(T,P,x_j)$ isobaric-isothermal thermodynamic *preferential interaction parameter*
$\eta_o(T,P,x_j)$ $(\rho_o/\mathscr{D})$
$\kappa_j^{o}(T,P)$ isothermal compressibility of the pure $j-$ solvent
$\kappa_o(T,P,x_{\alpha})$ isothermal compressibility of the mixed-solvent environment
$\mu_{\alpha}(T,P,x_{\alpha})$ chemical potential of the $\alpha-$ species
$\mu_{\alpha}^{*}(T,P,x_{\alpha})$ pseudo-chemical potential of the $\alpha-$ species
$\mu_{\alpha}^{R}(T,P,x_{\alpha})$ isobaric-isothermal residual chemical potential of the $\alpha-$ species
$\mu_i^{\ominus}(T,P,x_j)$ molar-based standard chemical potential of the $i-$ solute
$\rho_o(T,P,x_{\alpha})$ molar/molecular density of the system
$\zeta(T,P,x_{\alpha})$ the correlation length of the mixed-solvent environment

Sub- and super-scripts

c critical condition for the pure $j-$ solvent
faulty property associated with the incorrectly inverted $G_{ij}^{\infty}(T,P,x_j)$
o pure component
∞ infinite dilution in either an $\alpha-$ solvent or an $(\alpha+\beta)-$ mixed solvent
i solute species
IS ideal solution
j solvent species
k cosolvent species
IG ideal gas condition
IG_i special case of solute as an ideal gas $i-$ species
$LR-IS$ Lewis-Randall ideality, i.e., $\Delta_{\alpha\beta}(T,P,x_{\alpha})=0$
Q stability coefficient in terms of the second composition derivative of the excess Gibbs free energy of the mixed-solvent, i.e., $Q=kT\mathscr{D}$
R isobaric-isothermal residual property
r isochoric-isothermal residual property

we have recently proposed an elegant way to make such a connection through the statistical mechanics-based *fundamental structure making/-breaking functions* $\mathscr{S}_{\alpha\beta}(T,P,x_{\alpha})$ associated with any species in solution, [31,32] and consequently, provided the molecular thermodynamic interpretation leading to the eventual thermodynamic modeling of mixed-solvent systems.

Given the large body of experimental data on the solubility of natural products and synthetic pharmaceutical species (*aka* drugs), in this work we focus on their preferential solvation in a variety of mixed-solvent environments aimed at (*i*) characterizing the solvent effects on the solute solubility as a manifestation of their differential solvation abilities, (*ii*) revealing the rigorous macroscopic-to-microscopic relations between the variation of the Gibbs free energy of solute transfer $\Delta_{tr}g_i(T,P,x_j)$ — as the thermodynamic response to changes in mixed-solvent composition — and a precisely defined *universal preferential solvation function* $\mathscr{PS}(T,P,x_j)$, (*iii*) confronting the fundamentally-based formalism against a frequently invoked local composition approach while highlighting some persisting significant pitfalls, and (*iv*) illustrating the rigorous formalism through the analysis of the preferential solvation behavior of some additional pharmaceutical species in organic and aqueous-organic mixed-organic solvents under ambient conditions.

In pursuing our goals, in the Section 2, we describe the relevant molecular thermodynamics required to unravel rigorous formal

relations between the *fundamental structure making/breaking functions* $\mathscr{S}_{\alpha\beta}(T,P,x_\alpha)$ and the experimentally observed isothermal-isobaric composition dependence of the Gibbs free energy of solute transfer $\Delta_{tr}g_i(T,P,x_j)$. Next, we briefly discuss the foundations of a popular model of preferential solvation, inspired by the inverted Kirkwood-Buff integrals, and based on the local deviation of the solvent's mole fraction from its corresponding bulk counterpart. Therefore, in Section 3, we present a forensic analysis of the invoked Kirkwood-Buff inversion expressions for the implementation of the alluded preferential solvation model, identify some pervasive pitfalls and their associated root causes as well as their troubling physical consequences. Then, we present a comparison between the actual and the modelled behavior of some representative examples of preferential solvation in aqueous-organic mixed-solvents under ambient conditions to illustrate the troubling issues encountered in the implementation of the local composition model. Moreover, in Section 4, we illustrate the behavior of the *universal preferential solvation function* $\mathscr{PS}(T,P,x_j)$ for two sets of pharmaceutical solutes in organic mixed-solvents. Finally, in Section 5, we highlight the significance behind the analysis of preferential solvation, and provide some relevant observations and future outlook.

2. Fundamental Kirkwood-buff expressions relevant to preferential solvation thermodynamics

To make this formal analysis unambiguous and rigorous, we resort to previous developments interfacing chemical thermodynamics and statistical mechanics of fluid mixtures as embodied by the Kirkwood-Buff fluctuation theory of solutions [33] and its related solvation formalisms [34,35]

2.1. Universal preferential solvation function $\mathscr{PS}(T,P,x_j)$ in mixed-solvent environments according to the fundamental structure making/breaking functions $\mathscr{S}_{\alpha\beta}$

We have recently illustrated the inversion of the Kirkwood-Buff formalism, [36] involving $i-$ solutes at infinite dilution in $(j+k)-$ binary mixed-solvents according to the experimentally accessible thermodynamic properties. These quantities are the species partial molecular/molar volumes $(\widehat{v}_i^{\infty},\widehat{v}_j,\widehat{v}_k)$, the difussive stability coefficient $\mathscr{D}=\rho_o/\eta_o$, and the rate of change of the standard chemical potential of $i-$ solute in the mixed-solvent environment, $\left[\partial\mu_i^{\ominus}(T,P,x_j)/\partial x_j\right]_{TP}$, leading to the five relevant total correlation functions (*TCFI*'s, *aka* Kirkwood-Buff integrals), *i.e.*, G_{ij}^{∞}, G_{ik}^{∞}, G_{jk}, G_{kk}, G_{jj}, in terms of four *fundamental structure making/breaking functions* $\mathscr{S}_{\alpha\beta}$ [32]. In this analysis, we typically start with the first three functional $G_{\alpha\beta}(\widehat{v}_\alpha,\widehat{v}_\beta,\kappa_o,\eta_o)$ relations of the mixed-solvent environment which are then explicitly written in terms of $(\mathscr{S}_{kj},\mathscr{S}_{jk})$ as follows,

$$G_{jk}=kT\kappa_o-(1-\mathscr{S}_{kj})(1-\mathscr{S}_{jk})\eta_o^{-1} \tag{1}$$

$$G_{jj}=G_{jk}-\mathscr{S}_{kj}\rho_j^{-1} \tag{2}$$

$$G_{kk}=G_{jk}-\mathscr{S}_{jk}\rho_k^{-1} \tag{3}$$

where [31]

$$\begin{aligned}\mathscr{S}_{jk}(T,P,x_j)&=\rho_k(G_{kj}-G_{kk})\\&=1-\eta_o\widehat{v}_j\end{aligned} \tag{4}$$

$$\begin{aligned}\mathscr{S}_{kj}(T,P,x_j)&=\rho_j(G_{jk}-G_{jj})\\&=1-\eta_o\widehat{v}_k\end{aligned} \tag{5}$$

with, [37]

$$\begin{aligned}\eta_o&=\rho_o\Big/\left[1+\left(\partial\ln\gamma_j\Big/\partial\ln x_j\right)_{TP}\right]\\&=\rho_o/\mathscr{D}\end{aligned} \tag{6}$$

$$\rho_o=\lim_{x_i\to 0}\rho=\rho_j+\rho_k \tag{7}$$

$$\rho_j\widehat{v}_j+\rho_k\widehat{v}_k=1 \tag{8}$$

The last two *TCFI*'s, associated with the solvation of the infinitely dilute $i-$ solute, are then determined from the following thermodynamic equations linking the $i-$ solute partial molar volume at infinite dilution in the mixed solvent,

$$\widehat{v}_i^{\infty}=kT\kappa_o-\rho_j\widehat{v}_jG_{ij}^{\infty}-\rho_k\widehat{v}_kG_{ik}^{\infty} \tag{9}$$

with $\kappa_o=\lim_{x_i\to 0}\kappa$ denoting the isothermal compressibility of the mixed-solvent, and either the composition derivative $\left[\partial\mu_i^{\ominus}(T,P,x_j)/\partial x_j\right]_{TP}$ or its alternative $\left[\partial\ln(\widehat{\phi}_iz)^{\infty}/\partial x_j\right]_{TP}$ and $\left[\beta\partial\Delta_{tr}g_i(x_j)/\partial x_j\right]_{TP}$ representations (see below Eq. (16)), as follows [32]

$$\left[\partial\ln(\widehat{\phi}_iz)^{\infty}/\partial x_j\right]_{TP}=\rho_o\left(G_{ik}^{\infty}-G_{ij}^{\infty}\right)\left[1+\left(\partial\ln\gamma_j\Big/\partial\ln x_j\right)_{TP}\right] \tag{10}$$

In Eq. (10) we identify $\widehat{\phi}_i^{\infty}$, $z=P/kT\rho$, and γ_j as the fugacity coefficient of the $i-$ solute at infinite dilution, the compressibility factor, and the Lewis-Randall based activity coefficient of the $j-$ species in the mixed-solvent system, respectively. Thus, by solving the pair of Eqs. (9), (10), we immediately find the desired inversion expressions,

$$G_{ij}^{\infty}=kT\kappa_o-\widehat{v}_i^{\infty}-x_k\widehat{v}_k\mathscr{D}^{-1}\left[\partial\ln(\widehat{\phi}_iz)^{\infty}/\partial x_j\right]_{TP} \tag{11}$$

$$G_{ik}^{\infty}=kT\kappa_o-\widehat{v}_i^{\infty}+x_j\widehat{v}_j\mathscr{D}^{-1}\left[\partial\ln(\widehat{\phi}_iz)^{\infty}/\partial x_j\right]_{TP} \tag{12}$$

Moreover, by invoking the *universal preferential solvation function* $\mathscr{PS}(T,P,x_j)=\rho_o\left(G_{ik}^{\infty}-G_{ij}^{\infty}\right)$, [32,37] we can alternatively rewrite the last two expressions as follows,

$$G_{ij}^{\infty}=kT\kappa_o-\widehat{v}_i^{\infty}-x_k\widehat{v}_k\mathscr{PS} \tag{13}$$

$$G_{ik}^{\infty}=kT\kappa_o-\widehat{v}_i^{\infty}+x_j\widehat{v}_j\mathscr{PS} \tag{14}$$

Because the left-hand-side of Eq. (10) also reads as $\left[\partial\ln(\widehat{\phi}_iz)^{\infty}/\partial x_j\right]_{TP}=\left[\beta\partial\mu_i^{\ominus}(x_j)/\partial x_j\right]_{TP}$with $\beta=(kT)^{-1}$, we can immediately make contact with the experimentally available Gibbs free energy of solute transfer between two solvent environments, [38]

$$\begin{aligned}\Delta_{tr}g_i(T,P,x_j)&=\int_0^{x_j}\left(\partial\mu_i^{\ominus}/\partial x_j\right)_{TP}dx_j\\&=\mu_i^{\ominus}(T,P,x_j)-\mu_i^{\ominus}(T,P,x_j=0)\end{aligned} \tag{15}$$

so that, the required left-hand-side in Eq. (10) can be evaluated from the composition dependence of the experimentally available $\Delta_{tr}g_i(T,P,x_j)$, *i.e.*,

$$\left[\partial\ln(\widehat{\phi}_iz)^{\infty}/\partial x_j\right]_{TP}=\left[\beta\partial\Delta_{tr}g_i(x_j)/\partial x_j\right]_{TP} \tag{16}$$

Additionally, this macroscopic solvation quantity becomes rigorously expressed as a linear combination of differences of *fundamental structure making/breaking functions* $\mathscr{S}_{\alpha\beta}$, i.e.,

$$\begin{aligned}\left[\partial\ln(\widehat{\phi}_iz)^{\infty}/\partial x_j\right]_{TP}=&\left[x_k^{-1}\left(\mathscr{S}_{ik}^{\infty}-\mathscr{S}_{jk}\right)-x_j^{-1}\left(\mathscr{S}_{ij}^{\infty}-\mathscr{S}_{kj}\right)\right]\Big/\\&\left(1-x_k\mathscr{S}_{kj}-x_j\mathscr{S}_{jk}\right)\end{aligned} \tag{17}$$

where the denominator stays always positive, *i.e.*, $\mathscr{D}(T,P,x_j)=\left(1-x_k\mathscr{S}_{kj}-x_j\mathscr{S}_{jk}\right)^{-1}>0$ for any binary homogeneous stable phase [39]. Consequently, since the numerator and denominator of Eq. (17) comprise four *fundamental structure making/breaking functions*, ($\mathscr{S}_{ij}^{\infty}$,

$\mathscr{S}_{ik}^{\infty}$, $\mathscr{S}_{jk}$, $\mathscr{S}_{kj}$), the differential solute-induced microstructural perturbation of the solvent environment, *aka* the *universal preferential solvation function* $\mathscr{PS}(T,P,x_j)$, becomes described entirely in terms of a linear combination of the same state functions,

$$\mathscr{PS}(T,P,x_j) = \left(\mathscr{S}_{ik}^{\infty} - \mathscr{S}_{jk}\right) / x_k - \left(\mathscr{S}_{ij}^{\infty} - \mathscr{S}_{kj}\right) / x_j \tag{18}$$

with $\mathscr{S}_{i\alpha}^{\infty} = \rho_\alpha\left(G_{i\alpha}^{\infty} - G_{\alpha\alpha}\right)$ for $\alpha = j,k$.

Before proceeding with the next section, we must emphasize the significance of the described formalism in the context of the applications involving mixed-solvent systems in chemical processes, something that usually becomes lost in this type of studies. On the one hand, most studies of solvent effects focus on getting the composition profiles of some preferential solvation marker, followed by attempts to justify the outcome according to conjectured mechanisms and/or the balance of intervening solute-solvent versus solute-cosolvent interactions [40–42]. On the other hand, the above rigorous and general molecular-based approach characterized by Eqs. (15)–(18) does not depend on the type or nature of the intermolecular interactions, yet, it provides a direct and explicit link between the preferential solvation (output) and the tuning of the standard chemical potential of the solute (input) through changes in the composition of the mixed-solvent environment. In fact, from Eqs. (10)–(16), we can highlight the alluded connection as follows, (see additional discussion in §5)

$$\begin{aligned}\left[\partial\mu_i^{\ominus}(x_j)/\partial\mu_j(x_j)\right]_{TP} &= x_j\mathscr{PS}(T,P,x_j)\\ &= \Gamma_{ij}^{(x_i\to 0)}(T,P,x_j)\end{aligned} \tag{19}$$

where $\Gamma_{ij}^{(x_i\to 0)}(T,P,x_j)$ identifies the isobaric-isothermal thermodynamic *preferential interaction parameter* [32]. A step-by-step description of the determination of $\mathscr{PS}(x_j)$, $\delta_{ji}^0(x_j)$, $\delta_{ji}(x_j)$, $\mathscr{S}_{\alpha\beta}(x_j)$ and $\mathscr{S}_{i\alpha}^{\infty}(x_j)$ functions (outputs) according to the properly inverted Kirkwood-Buff integrals (inputs) is given in SI.4 of the Supplementary Information document.

2.2. Insights on a popular local composition approach to preferential solvation in mixed-solvent systems

The local composition ideas behind the modeling of solution thermodynamic non-idealities has been frequently invoked as a versatile tool for the *regression* of the Gibbs free energy of mixing since their inception by Wilson [43]. While the physical concept of local composition appears to be sound, and led to rather successful *correlations* of thermodynamic excess properties, [44–46] it cannot brush off the intrinsic drawback associated with its "local" domain size-dependent nature, despite numerous theoretical efforts [47–52]. Yet, Ben-Naim [53] was able to introduce a local composition-based definition of preferential solvation of an $i-$ solute in a mixed $(\alpha+\beta)-$ solvent system as a measure of the deviation of the local composition of the $\alpha-$ solvent in an arbitrary correlation volume $V_c(R_c^{i\alpha})$ centered at the $i-$ solute, from the corresponding global composition, *i.e.*,

$$x_{\alpha i}^{L} = \mathscr{N}_{i\alpha}(R_c^{i\alpha}) / z_i \tag{20}$$

where $z_i = \left[\mathscr{N}_{i\alpha}(R_c^{i\alpha}) + \mathscr{N}_{i\beta}(R_c^{i\beta})\right]$ identifies the near mixed-solvent coordinating neighbors for the $i-$ species. Thus, $\mathscr{N}_{i\alpha}(R_c^{i\alpha})$ and $\mathscr{N}_{i\beta}(R_c^{i\beta})$ represent the average number of $\alpha-$ solvent and $\beta-$ cosolvent within the solvation shell of radii $R_c^{i\alpha}$ and $R_c^{i\beta}$, typically with $R_c^{i\alpha} \neq R_c^{i\beta}$ leading to the *local compositions* described as the local mole fractions $x_{\alpha i}^{L} \neq x_{\beta i}^{L}$ under the obvious physical constraint $x_{\alpha i}^{L} + x_{\beta i}^{L} = 1$. To determine $\mathscr{N}_{i\alpha}(R_c^{i\alpha})$ and $\mathscr{N}_{i\beta}(R_c^{i\beta})$ according to the actual microstructure of the mixed-solvent system, Ben-Naim's approach assumes a plausible split of the Kirkwood-Buff integrals into two contributions, *i.e.*,

$$\begin{aligned}G_{i\alpha}(T,P,x_\alpha) &\equiv 4\pi\int_0^{\infty}\langle h_{i\alpha}(r_{i\alpha})\rangle_{\omega_i\omega_\alpha} r_{i\alpha}^2 dr_{i\alpha}\\ &= 4\pi\int_0^{R_c^{i\alpha}}\langle g_{i\alpha}(r_{i\alpha})\rangle_{\omega_i\omega_\alpha} r_{i\alpha}^2 dr_{i\alpha} - V_c(R_c^{i\alpha})\end{aligned} \tag{21}$$

according to the choice of the correlation radius $R_c^{i\alpha}$, which also defines the correlation volume $V_c^{i\alpha}(R_c^{i\alpha}) = 4\pi R_c^{i\alpha,3}/3$, where $\langle(\cdots)\rangle_{\omega_i\omega_\alpha} = \int(\cdots)d\omega_i d\omega_\alpha / \int d\omega_i d\omega_\alpha$ describes an orientational average over all relative orientations $(\omega_i\omega_\alpha)$ of the $i\alpha-$ pair.

In Eq. (21), we invoke the correlation radius $R_c^{i\alpha}$ rather than a generic R_c common to all $i\alpha-$ and $i\beta-$ pairs because, a properly defined (statistical mechanic-based) local mole fraction for the binary mixed-solvent requires the knowledge of all correlation radii $\left(R_c^{i\alpha}, R_c^{i\beta}\right)$ to fulfill relevant constraints regarding the balance of the local number of interactions [47,48] as extensively discussed by Lee et al. [49,50]. Consequently, Eq. (21) leads to the desired determination of the number of $\mathscr{N}_{i\alpha}(R_c^{i\alpha})$ pairs when ρ_α denotes the global number density of the $\alpha-$ solvent,

$$\mathscr{N}_{i\alpha}(R_c^{i\alpha}) \equiv 4\pi\rho_\alpha\int_0^{R_c^{i\alpha}}\langle g_{i\alpha}(r_{i\alpha})\rangle_{\omega_i\omega_\alpha} r_{i\alpha}^2 dr_{i\alpha} = \rho_\alpha G_{i\alpha} + \rho_\alpha V_c^{i\alpha}(R_c^{i\alpha}) \tag{22}$$

and finally, from Eqs. (20)–(22), the deviation of the local mole fraction of the $\alpha-$ solvent around the $i-$ solute from that of the bulk composition, *aka* the preferential solvation parameter $\delta_{\alpha i}\left(R_c^{i\alpha}, R_c^{i\beta}\right)$, becomes [37]

$$\begin{aligned}&\delta_{\alpha i}\left(R_c^{i\alpha}, R_c^{i\beta}\right) = x_{\alpha i}^{L}\left(R_c^{i\alpha}, R_c^{i\beta}, x_\alpha\right) - x_\alpha\\ &= \frac{x_\alpha x_\beta\left(G_{i\alpha}^{\infty} - G_{i\beta}^{\infty}\right) + x_\alpha x_\beta\left[V_c^{i\alpha}(R_c^{i\alpha}) - V_c^{i\beta}(R_c^{i\beta})\right]}{\left(x_\alpha G_{i\alpha}^{\infty} + x_\beta G_{i\beta}^{\infty}\right) + x_\alpha V_c^{i\alpha}(R_c^{i\alpha}) + x_\beta V_c^{i\beta}(R_c^{i\beta})}\end{aligned} \tag{23}$$

which will converge to Eq. 2.11 in Ref. [53] when setting $R_c = R_c^{i\alpha} = R_c^{i\beta}$ leading also to $V_c = V_c^{i\alpha} = V_c^{i\beta}$.

It becomes immediately obvious from Eq. (20) that the local composition depends on the size of the correlation volumes $\left(V_c^{i\alpha}, V_c^{i\beta}\right)$, a condition that spills over the definition of preferential solvation parameter $\delta_{\alpha i}\left(R_c^{i\alpha}, R_c^{i\beta}\right)$, Eq. (23), or its related $\delta_{\alpha i}(R_c)$. These issues have been avoided in Ben-Naim's original development, [53–55], through the first-order expansion around the $R_c^{-1}\to 0$ limiting condition, which led to the definition of the first-order preferential solvation parameter $\delta_{\alpha i}^0 \equiv x_\alpha x_\beta\left(G_{i\alpha}^{\infty} - G_{i\beta}^{\infty}\right)$. In contrast to Ben-Naim's $\delta_{\alpha i}^0$, the frequently invoked Marcus' implementation [27] for the determination of preferential solvation based on $\delta_{\alpha i}\left(R_c^{i\alpha} = R_c^{i\beta} = R_c\right)$, Eq. 2.11 in Ref. [53],

$$\begin{aligned}&\delta_{\alpha i}(R_c,x_\alpha) = x_{\alpha i}^{L}(R_c,x_\alpha) - x_\alpha\\ &= x_\alpha x_\beta\left(G_{i\alpha}^{\infty} - G_{i\beta}^{\infty}\right)\Big/\left(x_\alpha G_{i\alpha}^{\infty} + x_\beta G_{i\beta}^{\infty} + V_c\right)\end{aligned} \tag{24}$$

not only does violate the local balance conditions, but also requires an additional expression for the estimation of the composition dependent correlation volume $V_c\left(\widehat{v}_i^{\infty}, x_{\alpha i}^{L}, x_\alpha\right)$ such as Eq. 8a-b in Ref. [56].

We must also emphasize that, regardless of the procedure used in the estimation of $V_c\left(\widehat{v}_i^{\infty}, x_{\alpha i}^{L}, x_\alpha\right)$, Eq. (24) involves tacitly a source of potential troubles given the lack of explicit enforcement of the splitting requirement (see also §3 and §5),

$$G_{i\alpha}(T,P,x_\alpha) = 4\pi\int_0^{R_c^{i\alpha}>\zeta}\langle g_{i\alpha}(r_{i\alpha})\rangle_{\omega_i\omega_\alpha} r_{i\alpha}^2 dr_{i\alpha} - V_c\left(R_c^{i\alpha} > \zeta\right) \tag{25}$$

where ζ defines the correlation length of the mixed-solvent environment, i.e., the distance travelled by the solute-induced perturbation of the microstructure of the solvent environment around it [57]. It becomes obvious that the first-order preferential solvation parameter $\delta_{\alpha i}^0 \equiv x_\alpha x_\beta\left(G_{i\alpha}^{\infty} - G_{i\beta}^{\infty}\right)$ fulfills this condition automatically. However, we

must also be mindful that either the condition $R_c^{i\alpha} > \zeta$ might be unattainable when dealing with highly compressible solvent environments, [26] or when the resulting $R_c^{i\alpha} = \sqrt[3]{3V_c\left(\widehat{v}_i^{\infty}, x_{\alpha i}^{L}, x_\alpha\right)/4\pi}$ from the iterative regression of Eq. (24) translates into $R_c^{i\alpha} \ll \zeta$ as suggested by the microstructural information from molecular simulation of aqueous systems [58,59]

3. Critical analysis of the reliability of a frequently used local composition-based preferential solvation formalism

In this section, we first discuss the risks associated with the proverbial *black box* application of modeling tools such as Marcus' implementation of the local composition-based approach to preferential solvation in mixed-solvent systems [60–63]. Then, we identify explicitly a pair of persisting pitfalls in its application, which have compromised the outcome of a great deal of published work on the modeling of preferential solvation (see SI.1 and SI.2 in the Supplementary Information), a fact that has remained so far unnoticed in the literature.

3.1. Subtle pitfalls in the local composition-based approach to preferential solvation leading to non-sensical and unphysical results

As indicated previously in §2.1 of Ref. [37], we frequently find that the local composition approach to the assessment of preferential solvation, such as that in Ref. [56], has been used as a routine *gadget* to determine the deviation parameter $\delta_{\alpha i}(R_c, x_\alpha) = x_{\alpha i}^{L}(R_c, x_\alpha) - x_\alpha$ according to Eq. (24) in the previous section. Unfortunately, its *black box* approach, in conjunction with the iterative nature of the underlying R_c evaluation, [64] could lead to either subtle thermodynamic inconsistencies, unphysical results or both simultaneously, while unbeknown to the modeling practitioners.

On the one hand, we have previously discussed and illustrated the case of a homogeneous real mixture whose thermodynamic modeling resulted in an incompatible liquid-liquid phase split that led to unsupported interpretations of preferential solvation [37]. On the other hand, no matter how we approached the calculation of the domain radius R_c, or its correlation volume counterpart $V_c(R_c)$, the resulting preferential solvation parameter $\delta_{\alpha i}(R_c, x_\alpha) = x_{\alpha i}^{L}(R_c, x_\alpha) - x_\alpha$ should always result in a positive local mole fraction $x_{\alpha i}^{L}(R_c, x_\alpha)$; otherwise, there would be something seriously wrong with the invoked local composition formalism. Unfortunately, while unthinkable in the chemical thermodynamic literature, we have encountered a rather alarming number of recently published research regarding solvent effects on the solubility of natural and pharmaceutical species (as discussed and sampled in SI.1 and SI.2 of the Supplementary Information) where the tabulated data and/or displayed illustrations comprise $\delta_{\alpha i}(R_c, x_\alpha) < 0$ that lead to physically meaningless negative local compositions, $x_{\alpha i}^{L}(R_c, x_\alpha) = \delta_{\alpha i}(R_c, x_\alpha) + x_\alpha < 0$. In fact, in the Tables SI-1 and SI-2 of the Supplementary Information, we collect a sample of citations covering a large number of published work where we have identified the unnoticed unphysical results caused by the failure to recognize the material instability (*i.e.*, phase separation), the occurrence of $x_{\alpha i}^{L}(R_c, x_\alpha) < 0$, and the manifestation of both issues simultaneously.

Given the seriousness of these issues, and prior to any comparison of preferential solvation methodologies, we must pinpoint the origin of the problem, one that we have identified as a crucial misprint in the local composition formalism presented in Ref. [61] which has remained unnoticed, and consequently, has propagated into hundreds of associated publications up to these days. Moreover, we must highlight another frequent overlooked thermodynamic condition associated with the material stability of the mixed-solvent environment, [39] whose effects on the calculated preferential solvation translate into discontinuous behaviors and generate somewhat bizarre interpretations [37].

3.2. Root cause of the unnoticed pitfalls in the local composition approach to the preferential solvation parameter $\delta_{ji}(R_c, x_j)$

After a thorough search in the related literature, and a *forensic* analysis of the tabulated data, we found the first clue about the origin of the unexpected behavior in the published $\delta_{ji}(R_c, x_j)$: most of the affected publications invoking Marcus' approach — Eq. (24) in conjunction with the composition dependence of the correlation volume $V_c\left(\widehat{v}_i^{\infty}, x_{ji}^{L}, x_j\right)$ given in Ref. [56] — follow literally either Eqs. 5.33a-5.33b of Ref. [60], Eq. (6) of Ref. [61], Eqs. 2.51–2.52 of Ref. [62] or Eqs. 6.25a-6.25b of Ref. [63]. The second citation appears to be the one mostly invoked in the affected publications (about 165 publications to date, as compiled in the Supplementary Information) which became the source of propagation of a faulty inversion expression in the invoked Kirkwood-Buff formalism.

More specifically, the fault in either Eq. 5.33b of Ref. [60] or Eq. (6) of Ref. [61], initially thought to be just a misprint, reads in our notation as follows,

$$\begin{aligned} G_{ij}^{\infty,faulty} &= kT\kappa_o - \widehat{v}_i^{\infty} + x_k\widehat{v}_k\mathscr{D}^{-1}\left[\partial\ln(\widehat{\phi}_i z)^{\infty}/\partial x_j\right]_{TP} \\ &= G_{ij}^{\infty} + 2x_k\widehat{v}_k\mathscr{D}^{-1}\left[\partial\ln(\widehat{\phi}_i z)^{\infty}/\partial x_j\right]_{TP} \end{aligned} \tag{26}$$

where $G_{ij}^{\infty,faulty}$ and G_{ij}^{∞} denote the misprinted and correct quantities, respectively, after we identify the equivalences between the thermodynamic functions $\mathscr{D} = Q/kT$ and $\left[kT\partial\ln(\widehat{\phi}_i z)^{\infty}/\partial x_j\right]_{TP} = \left[\partial\Delta_{tr}g_i(x_j)/\partial x_j\right]_{TP}$ in Refs. [60,61]. A direct comparison between Eqs. (26) and (11) identifies the wrong sign in the last term at the first line of Eq. (26). In fact, this error might become immediately obvious when we perform the difference between Eqs. (5), (6) in Ref. [61] to recover the original Eq. (10). Instead, we get the following outcome,

$$\left[\partial\ln(\widehat{\phi}_i z)^{\infty}/\partial x_j\right]_{TP} = \left(G_{ik}^{\infty} - G_{ij}^{\infty,faulty}\right)\left[1 + \left(\partial\ln\gamma_j/\partial\ln x_j\right)_{TP}\right]\left(x_j\widehat{v}_j - x_k\widehat{v}_k\right)^{-1} \tag{27}$$

which satisfies the correct Eq. (10) only when $x_j = 1$. Moreover, the introduction of $\left(G_{ij}^{\infty,faulty} - G_{ik}^{\infty}\right)$ into the numerator of the preferential solvation parameter, Eq. (24), will generate a faulty preferential solvation parameter, as derived in Appendix A, *i.e.*,

$$\delta_{ji}^{faulty}(x_j) = \frac{\delta_{ji}(x_j)\left(x_jG_{ij}^{\infty} + x_kG_{ik}^{\infty} + V_c\right) + 2x_jx_k^2\widehat{v}_k\mathscr{D}^{-1}\left[\partial\ln(\widehat{\phi}_i z)^{\infty}/\partial x_j\right]_{TP}}{\left(x_jG_{ij}^{\infty,faulty} + x_kG_{ik}^{\infty} + V_c^{faulty}\right)} \tag{28}$$

Similarly, for the equivalent composition derivatives defining the rate of change of the Gibbs free energy of solute transfer, *i.e.*,

$$\begin{aligned} \left[\partial\Delta_{tr}g_i(x_j)/\partial x_j\right]_{TP}^{faulty} &= \left[\partial\Delta_{tr}g_i(x_j)/\partial x_j\right]_{TP}\left(\rho_j\widehat{v}_j - \rho_k\widehat{v}_k\right) \\ \left[\partial\ln(\widehat{\phi}_i z)^{\infty}/\partial x_j\right]_{TP}^{faulty} &= \left[\partial\ln(\widehat{\phi}_i z)^{\infty}/\partial x_j\right]_{TP}\left(\rho_j\widehat{v}_j - \rho_k\widehat{v}_k\right) \end{aligned} \tag{29}$$

In summary, the use of the incorrect input $G_{ij}^{\infty,faulty}$ (*i.e.*, Eq. (26)) rather than G_{ij}^{∞} (*i.e.*, Eq. (11)) in the calculation of the preferential solvation parameter $\delta_{ji}(R_c, x_j)$, Eq. (24) and concomitant correlation volume $V_c\left(\widehat{v}_i^{\infty}, x_{ji}^{L}, x_j\right)$, results in the iteration of Eq. (28) rather than Eq. (24) and leads always to incorrect, and frequently, unphysical outcomes (see §3.3 below). Likewise, the use of $G_{ij}^{\infty,faulty}$ generates a significant deviation from the original input given by Eq. (16), with a magnitude described by Eq. (29), and consequently, we will not recover the starting experimental data for the composition slope of the Gibbs free energy of solute transfer, $\left[\partial\Delta_{tr}g_i(x_j)/\partial x_j\right]_{TP}$. In fact, as we discuss in Appendix A, the involvement of $G_{ij}^{\infty,faulty}$ rather than G_{ij}^{∞} implies that the calculation of

$\delta_{ji}(R_c, x_j)$ through Eq. (24) comprises actually $\left[\partial \Delta_{tr} g_i(x_j)/\partial x_j\right]_{TP}^{faulty}$ as an implicitly input, characterized by $\left[\partial \Delta_{tr} g_i(x_j \to small)/\partial x_j\right]_{TP}^{faulty} > 0$ with a negative slope in contrast to the $\left[\partial \Delta_{tr} g_i(x_j \to small)/\partial x_j\right]_{TP}^{experimental} < 0$ with a positive slope (*e.g.*, see Figs. A1-A2). Moreover, and for the same reason, Eq. (28) will predict a first-order preferential solvation parameter $\delta_{ji}^{0,faulty} = x_j x_k \left(G_{ij}^{\infty,faulty} - G_{ik}^{\infty}\right)$ that deviates from the intended $\delta_{ji}^{0} \equiv x_j x_k \left(G_{ij}^{\infty} - G_{ik}^{\infty}\right)$ as follows,

$$\delta_{ji}^{0,faulty} = \delta_{ji}^{0} + 2x_j x_k^2 \hat{v}_k \mathscr{D}^{-1} \left[\partial \ln(\hat{\phi}_i z)^{\infty}/\partial x_j\right]_{TP} \tag{30}$$

Although Eqs. (26)–(30) are rigorous theoretical expressions linking the expected answer with the faulty outcome, in the next section we will provide a few examples to illustrate graphically the magnitude and consequences of the application of the incorrectly inverted Kirkwood-Buff integral $G_{ij}^{\infty\,faulty}$ according to the experimentally available data.

3.3. Illustration of the forensic analysis on the tabulated data underlying the faulty preferential solvation parameter $\delta_{ji}^{faulty}(R_c, x_j)$

To illustrate the issue identified in the previous section, resulting from the wrong sign in the third term of the Kirkwood-Buff inverted $G_{ij}^{\infty}(x_j, T, \kappa_o, \mathscr{D}, \hat{v}_i, \hat{v}_k)$, in what follows, we proceed with the calculations of the quantities leading to the desired preferential solvation parameter $\delta_{ji}(R_c, x_j)$. For that purpose, we choose a pair of examples from the cited literature in the Supplementary Information, which identified directly either Ref. [60] or [61] as the source of the working equations, and invoked precisely the same thermodynamic input for the composition dependent $(\kappa_o, \mathscr{D}, \hat{v}_i, \hat{v}_j, \hat{v}_k, \left[\partial \Delta_{tr} g_i(x_j)/\partial x_j\right]_{TP})$ in the study of those systems.

For the first illustration, we have chosen from Table SI-1 of the Supplementary Information the system curcumin (i) in ethanol (j) + water (k) mixed-solvent at ambient conditions as studied in Ref. [65]

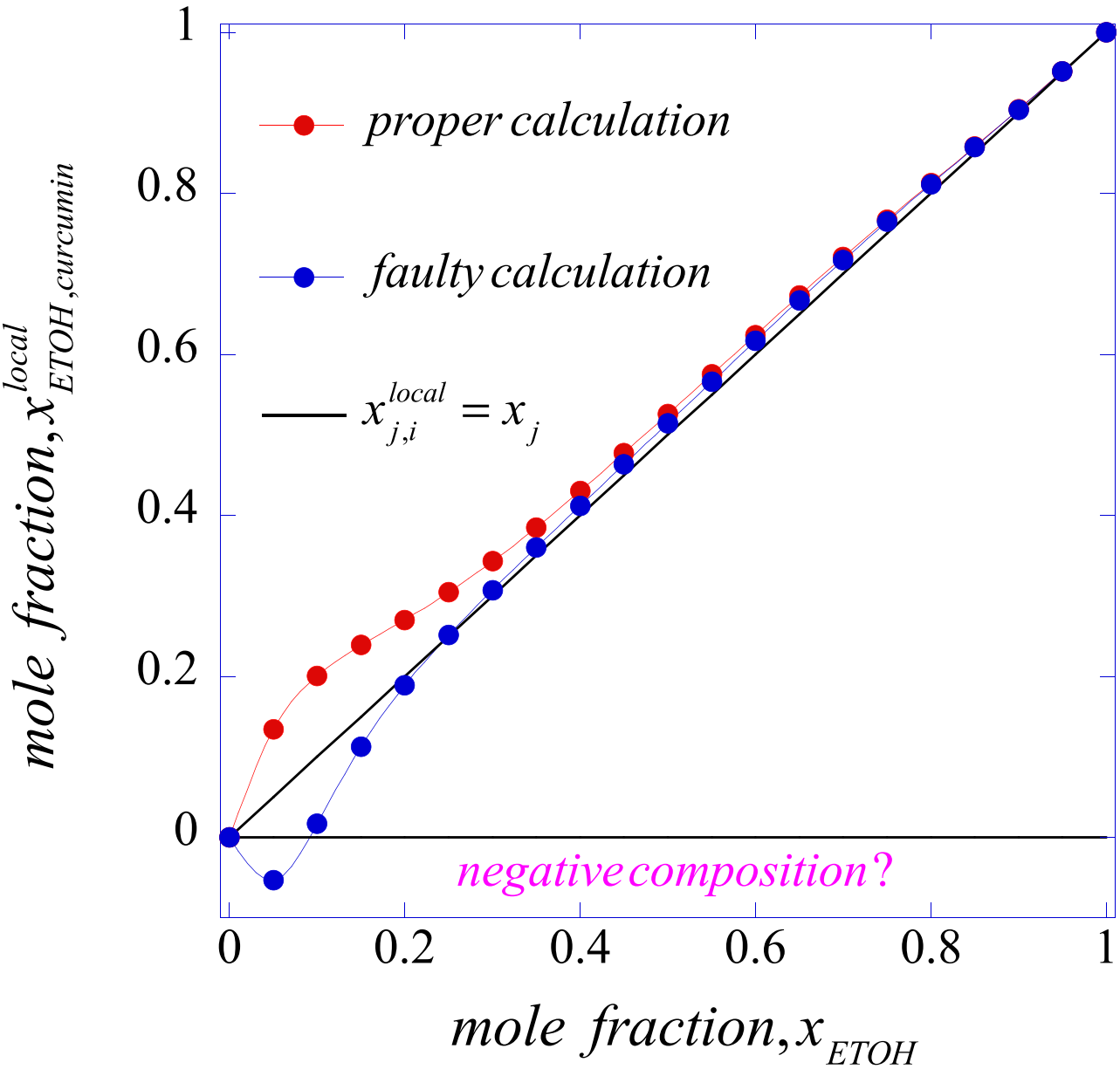

Fig. 1. Local ethanol mole fraction around curcumin as a function of the ethanol bulk mole fraction for the curcumin (i) in ethanol (j) + water (k) mixed-solvent at ambient conditions as studied in Ref. [65]. Comparison of outcomes between the correct and the faulty inverted Kirkwood-Buff integrals, and a highlight of the meaningless negative composition.

whose Fig. 7 and Table S17 describe negative local compositions. Our analysis in Figs. 1, 2 provides the behavior of the local composition of ethanol around the curcumin solute in the mixed-solvent environment, and its deviation from the bulk composition, to highlight the contrasting outcomes between the faulty and the correct implementations of the local composition approach to preferential solvation. According to the proper implementation, Fig. 1 indicates that curcumin induces an enhancement of the local concentration of ethanol relative to its bulk counterpart, $x_{j,i}^{L} > x_j$, over the entire range of composition. This behavior becomes more evident in Fig. 2, where we also plot the first-order preferential solvation parameter $\delta_{j,i}^{0}(x_j)$ defined by Ben-Naim [53]. These two plots suggest that the proper implementation of Marcus' approach [60,61] will lead to the preferential solvation of the curcumin solute by water, a conclusion also supported by the outcomes from Ben-Naim's preferential solvation parameter $\delta_{j,i}^{0}(x_j)$.

For the second illustration, we have chosen from Table SI-2 of the Supplementary Information the system 5-nitrosalicylic acid (i) in acetonitrile (j) + water (k) as studied in Ref. [66] whose Fig. 3 and Table S6 describe not only *negative local solvent compositions*, but also meaningless outcomes within the miscibility gap of the mixed-solvent. In Figs. 3, 4 we illustrate the behavior of the local composition of acetonitrile around the 5-nitrosalicylic acid and its deviation from the bulk composition in the mixed-solvent environment. In these comparisons between the faulty and the correct determinations of the local composition approach to preferential solvation, we highlight the miscibility gap and the fact that 5-nitrosalicylic acid actually induces an enhancement of the local concentration of acetonitrile relative to its bulk counterpart, $x_{j,i}^{L} > x_j$, over the entire range of composition where the mixed-solvent exhibits a stable phase. In other words, the correct implementation of the preferential solvation approaches of Marcus and Ben-Naim predicts a significant preferential solvation of the 5-nitrosalicylic acid solute by water. Unfortunately, this behavior is interrupted by

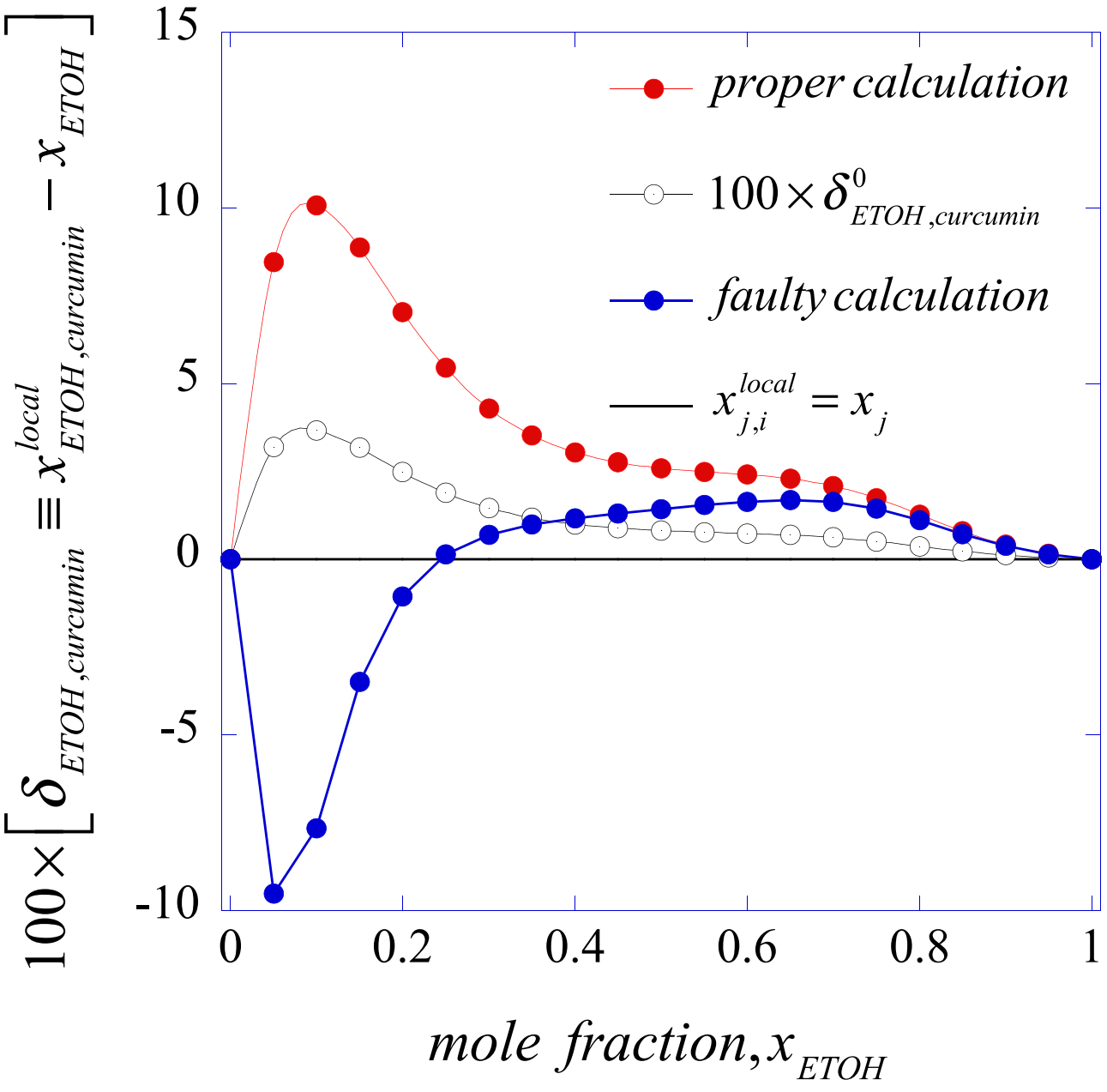

Fig. 2. Deviation of the local mole fraction of ethanol around curcumin from its bulk value in comparison with the corresponding first-order preferential solvation parameter as a function of the bulk mole fraction of ethanol for the curcumin (i) in ethanol (j) + water (k) mixed-solvent at ambient conditions as studied in Ref. [65].

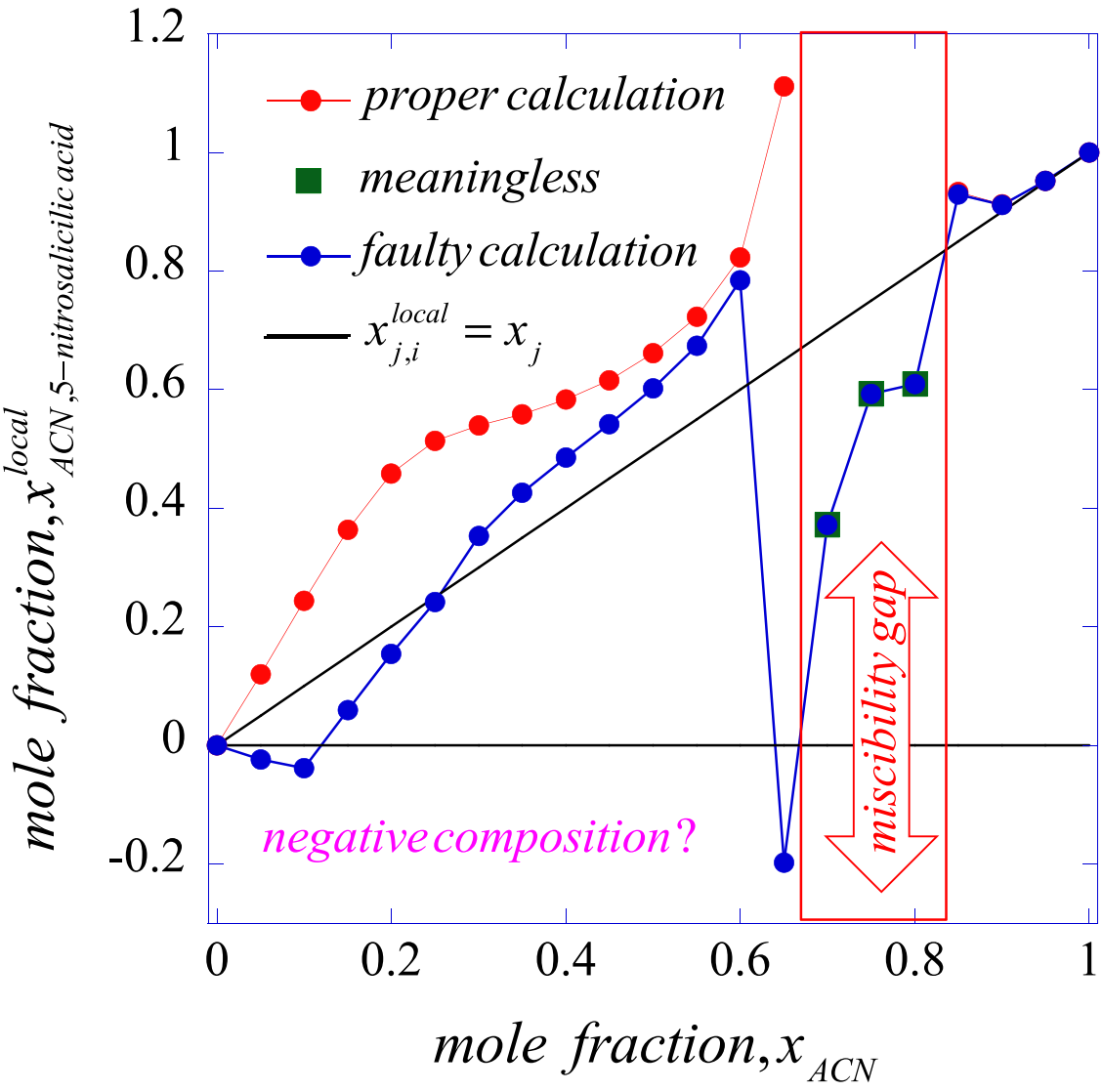

Fig. 3. Local acetonitrile mole fraction around 5-nitrosalicylic acid as a function of the acetonitrile bulk mole fraction for the system 5-nitrosalicylic acid (i) in acetonitrile (j) + water (k) as studied in Ref. [66]. Comparison of outcomes between the correct and the faulty inverted Kirkwood-Buff integrals, and highlight of meaningless compositions and outcome within the unstable region.

the presence of a solubility gap in the model acetonitrile (j) + water (k) mixed-solvent. In fact, as discussed elsewhere [37] and section SI.3 in the Supplementary Information, the real acetonitrile (j) + water (k) mixed-solvent system does not exhibit miscibility gap at ambient conditions; what we observe here is the manifestation of an inaccurate description of the composition dependence of the Gibbs free energy invoked in the original study.

Note that, as the concentration of the $k-$ cosolvent decreases, the faulty outcome for the local solvent composition around the solute and its deviation from the bulk, approaches the correct results. This behavior is the expected one considering that, according to Eq. (26),

$$G_{ij}^{\infty\,faulty}(x_j \to 1) \to G_{ij}^{\infty} = kT\kappa_o - \widehat{v}_i^{\infty} - x_k \widehat{v}_k \mathscr{D}^{-1}\left[\partial \ln(\widehat{\phi}_i z)^{\infty}/\partial x_j\right]_{TP} \tag{31}$$

Moreover, from Eq. (28) the faulty preferential solvation parameter $\delta_{ji}^{faulty}(x_j)$ will approach the correct value, *i.e.*, (see Appendix A)

$$\delta_{ji}^{faulty}(x_j \to 1) \to \delta_{ji}(x_j) \tag{32}$$

Otherwise, as the concentration of the $j-$ solvent decreases, the error from the faulty implementation increases to reach the largest limiting value, that according to Eq. (26), is given by

$$G_{ij}^{\infty\,faulty}(x_j \to 0) = G_{ij}^{\infty} + 2v_o \mathscr{D}^{-1}\left[\partial \ln(\widehat{\phi}_i z)^{\infty}/\partial x_j\right]_{TP} \tag{33}$$

This behavior becomes even more evident when plotting the composition dependence of the $\left[\partial \Delta_{tr} g_i(x_j)/\partial x_j\right]_{TP}$ according to Eq. (27), as illustrated in Figs. A1, A2 in Appendix A, where we display the comparison between the input $\left[\partial \Delta_{tr} g_i(x_j)/\partial x_j\right]_{TP}^{experimental}$ from the regression of the experimental Gibbs free energy of transfer, and the corresponding outcome $\left[\partial \Delta_{tr} g_i(x_j)/\partial x_j\right]_{TP}^{faulty}$ resulting from using the faulty inversion of the Kirkwood-Buff expression, *i.e.*, Eq. (26) rather than Eq. (11). These pictures also provide a hint on the significant drop of the calculated preferential solvation parameter $\delta_{ji}^{faulty}(x_j \to 0)$ that frequently triggers the prediction of a *negative local solvent composition, i.e.*, it actually involves implicitly a $\left[\partial \Delta_{tr} g_i(x_j \to small)/\partial x_j\right]_{TP}^{faulty} > 0$ in contrast

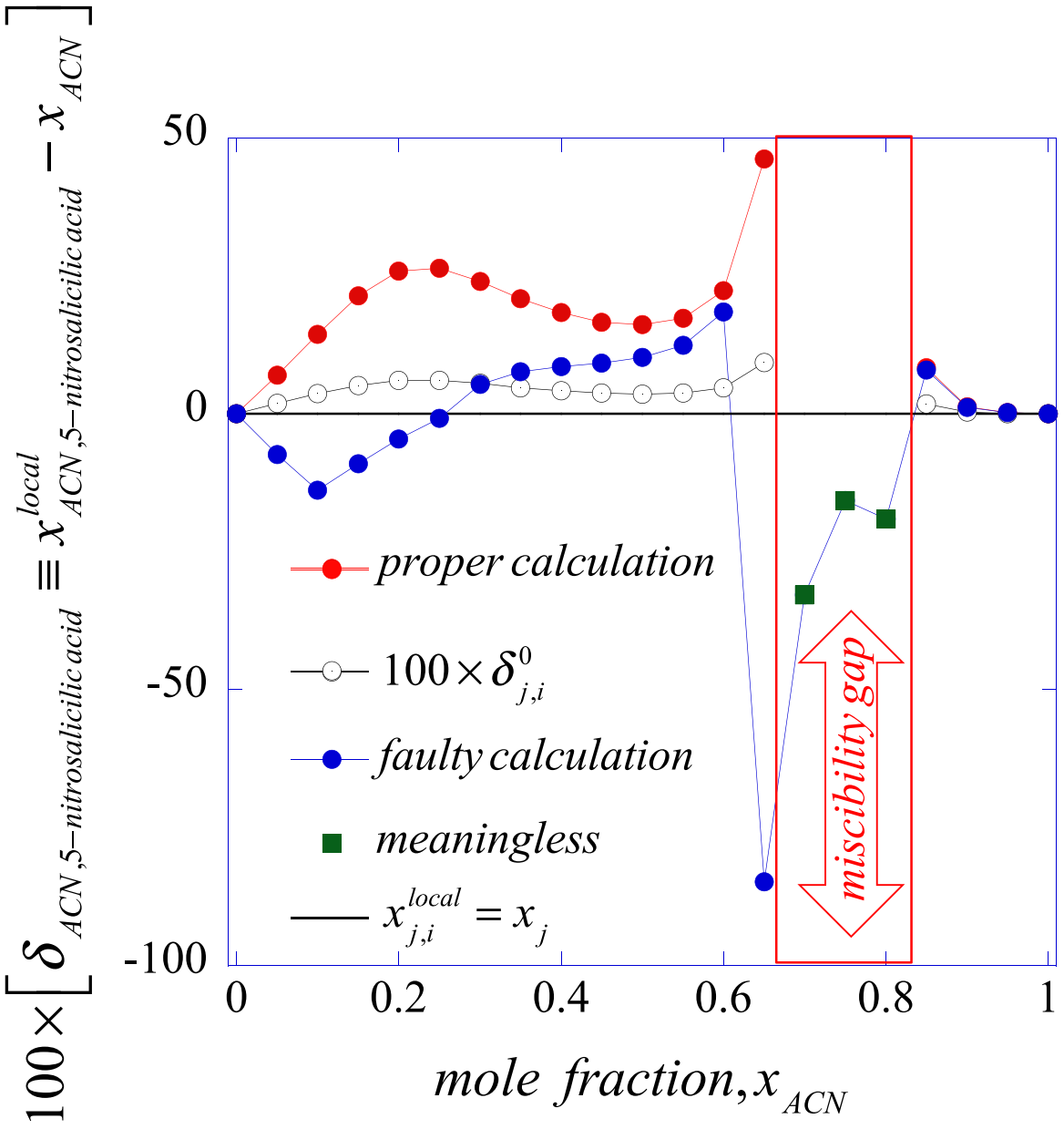

Fig. 4. Deviation of the local mole fraction of acetonitrile mole fraction around 5-nitrosalicylic acid from its bulk value in comparison with the corresponding first-order preferential solvation parameter as a function of the acetonitrile bulk mole fraction for the 5-nitrosalicylic acid (i) in acetonitrile (j) + water (k) mixed-solvent as studied in Ref. [66], and a highlight of the meaningless outcome within the unstable region.

to the $\left[\partial\Delta_{tr}g_i(x_j\to small)/\partial x_j\right]^{experimental}_{TP}<0$, as well as the approaching behavior described by Eq. (32).

4. Analysis of the preferential solvation behavior of pharmaceuticals in some organic mixed-solvent systems

In this section, we interrogate the isobaric-isothermal differential solute-induced microstructural perturbation of the mixed-solvent environment according to available experimental data, illustrate the behavior of the four *fundamental structure making/breaking functions* $\mathscr{S}_{\alpha\beta}(T,P,x)$, and link them to a descriptor of the solvent-cosolvent intermolecular interaction asymmetry according the methodology discussed in §2.1. Note that according to its definition, the *fundamental structure making/breaking function* manifests as one of the following three possible scenarios, *i.e.*, [31,57,67].

$$\mathscr{S}_{\alpha\beta}=\rho_\beta\left(G_{\alpha\beta}-G_{\beta\beta}\right)\begin{cases}>0\to\alpha\text{strengthen}\beta-\text{microstructure}\\=0\to\alpha\text{doesnotperturb}\beta-\text{microstructure}\\<0\to\alpha\text{weakens}\beta-\text{microstructure}\end{cases}\tag{34}$$

with $\mathscr{S}_{\alpha\beta}\neq\mathscr{S}_{\beta\alpha}$ so that, the *fundamental preferential solvation function* $\mathscr{PS}(T,P,x_j)$, Eq. (18), can be interpreted as a linear combination of two differences of *fundamental structure making/breaking functions,* i.e., $\left(\mathscr{S}^{\infty}_{ik}-\mathscr{S}_{jk}\right)$ and $\left(\mathscr{S}^{\infty}_{ij}-\mathscr{S}_{kj}\right)$, two functions that measure unambiguously the contrasting environment between the $\alpha-$ solvent and the $\beta-$ cosolvent around the $i-$ solute. On other words, $\mathscr{PS}(T,P,x_j)$ describes the interplay between the perturbation of the $k-$ cosolvent induced by the solute-solvent $(i,j)-$ pair of species in contrast to the perturbation of the $j-$ solvent induced by the solute-cosolvent $(i,k)-$ pair of species.

Some caution should be placed in the determination of total Kirkwood-Buff integrals associated with the microstructure of the

mixed-solvent environment, Eqs. (1)–(3), to attain the proper answers while avoiding apparent divergencies as the $\alpha-$ species (*i.e.*, solvent or cosolvent) approaches infinite dilution. In fact, Eqs. (1)–(3) might exhibit indeterminate $0/0-$ forms at the two infinite dilution conditions, whose rigorous limiting behavior define the osmotic second virial coefficient of the $\alpha-$ species $B_{\alpha}^{*,\rho}(T,P)$ in the density expansion of the associated absolute activity $\lambda_{\alpha}(T,\rho_{\alpha}) \equiv \rho_{\alpha}\widehat{\phi}_{\alpha}z$, [68]

$$\begin{aligned} &\lim_{x_{\alpha}\to 0} G_{\alpha\alpha}(T,P,x_{\alpha}) = -2B_{\alpha}^{*,\rho}(T,P) \\ &= kT\kappa_{\beta}^{o} - 2\widehat{v}_{\alpha}^{\infty} + v_{\beta}^{o}\left[1-(\partial \ln\gamma_{\alpha}/\partial x_{\alpha})_{TPx}^{\infty}\right] \end{aligned} \tag{35}$$

Obviously, at the pure component limit, Eqs. (1)–(3) must converge to the corresponding pure component behavior a follows,

$$\lim_{x_{\alpha}\to 1} G_{\alpha\alpha}(T,P,x_{\alpha}) = kT\kappa_{\alpha}^{o} - v_{\alpha}^{o} \tag{36}$$

for $\alpha = j,k$, so that $G_{jk}(T,P,x_j)$ fulfill the following limiting behaviors,

$$\begin{aligned} &\lim_{x_j\to 1} G_{jk}(T,P,x_j) = kT\kappa_{j}^{o} - \widehat{v}_{k}^{\infty} \\ &\lim_{x_j\to 0} G_{jk}(T,P,x_j) = kT\kappa_{k}^{o} - \widehat{v}_{j}^{\infty} \end{aligned} \tag{37}$$

Moreover, we can also make the following observations regarding the relative $i-$ solute to $\alpha-$ solvent induced perturbations of the $\beta-$ cosolvent environment, i.e.,

$$\left(\mathscr{S}_{i\beta}^{\infty} - \mathscr{S}_{\alpha\beta}\right) > 0 \begin{cases} \mathscr{S}_{i\beta}^{\infty} > \mathscr{S}_{\alpha\beta} > 0 \\ \mathscr{S}_{i\beta}^{\infty} > 0 \text{and} \mathscr{S}_{\alpha\beta} < 0 \\ \mathscr{S}_{\alpha\beta} < \mathscr{S}_{i\beta}^{\infty} < 0 \to \left|\mathscr{S}_{\alpha\beta}\right| > \left|\mathscr{S}_{i\beta}^{\infty}\right| \end{cases} \tag{38}$$

$$\left(\mathscr{S}_{i\beta}^{\infty} - \mathscr{S}_{\alpha\beta}\right) = 0 \to \mathscr{S}_{i\beta}^{\infty} = \mathscr{S}_{\alpha\beta} \underset{>}{\overset{\leq}{=}} 0 \tag{39}$$

$$\left(\mathscr{S}_{i\beta}^{\infty} - \mathscr{S}_{\alpha\beta}\right) < 0 \begin{cases} \mathscr{S}_{\alpha\beta} > \mathscr{S}_{i\beta}^{\infty} > 0 \\ \mathscr{S}_{i\beta}^{\infty} < 0 \text{and} \mathscr{S}_{\alpha\beta} > 0 \text{with} \left|\mathscr{S}_{i\beta}^{\infty}\right| > \mathscr{S}_{\alpha\beta} \\ \mathscr{S}_{i\beta}^{\infty} < \mathscr{S}_{\alpha\beta} < 0 \to \left|\mathscr{S}_{\alpha\beta}\right| < \left|\mathscr{S}_{i\beta}^{\infty}\right| \end{cases} \tag{40}$$

where the exchange of $\alpha \leftrightarrow \beta$ in Eqs. (38)–(40) provides the counterparts for the relative solute to cosolvent-induced perturbations of the solvent environment.

Finally, for the estimation of the isothermal compressibility $\kappa_o(x_j)$ of the mixed-solvent environment we have invoked the following ideal solution approximation [69,70].

$$\kappa_o(T,P,x_j) \cong \rho_j v_j^o \kappa_j^o + \rho_k v_k^o \kappa_k^o \tag{41}$$

with $\rho_{\alpha} = x_{\alpha}/\left(x_j v_j^o + x_k v_k^o\right)$, while for the partial molar volume $\widehat{v}_i^{\infty}(x_j)$, we adopt the suggested $\widehat{v}_i^{\infty}(x_j) \approx v_i^o$ approximation given the lack of experimental data (see also the relevant discussion in §5) [61].

4.1. Illustration of the preferential solvation of a representative pharmaceutical solute in a few potential organic mixed-solvent environments

For an instructive example of preferential solvation in binary mixed-solvents, we chose dehydroepiandrosterone acetate (*DHEA-A*) as a representative pharmaceutical solute, a more soluble form of *DHEA,* [71] known as an intermediate in the synthesis of estrogen and testosterone [72]. Because its solubility in a few neat organic and binary mixed-solvent environments has been recently determined along a few isotherms under ambient pressure, [73,74] we will take advantage of these data to characterize its preferential solvation according to our fundamentally-based formalism. More specifically, here we characterize the differential *DHEA-A* induced microstructural perturbation of the mixed-solvent environment along the $T = 313K$ isotherm under ambient pressure.

For that purpose, we extract the five total correlation functions integrals — G_{ij}^{∞}, G_{ik}^{∞}, G_{jk}, G_{kk}, and G_{jj} — through the inversion of the Kirkwood-Buff expressions according to the regressed experimental data available for the systems *DHEA-A* (i) + ethyl acetate (j) + k-cosolvent, *i.e.*, (a) the isothermal-isobaric Gibbs free energy of transfer of the $i-$ solute at infinite dilution in binary mixtures of the solvent ethyl acetate with either methanol, ethanol, or isopropanol as the cosolvent, $\Delta_{tr}g_i(T,P,x_j)$, [75] leading to the required $\left[\partial\Delta_{tr}g_i(x_j)/\partial x_j\right]_{TP}$ in Eqs. (11), (12), (b) the partial molar volumes $\widehat{v}_{\alpha}$ of the ethyl acetate (j) + k-cosolvent systems are determined using volumetric data from Ref. [76] for ethanol as well as Ref. [77] for methanol and isopropanol as the k-cosolvent, respectively, (c) the material stability coefficient $\mathscr{D}$ according to the excess Gibbs free energy of the mixed-solvent systems, [78] (d) the isothermal compressibility κ_o of the environment, and (e) the partial molar volume $\widehat{v}_i^{\infty}$. The last two properties are not needed for the determination of the preferential solvation function $\mathscr{PS}(T,P,x_j) = \rho_o\left(G_{ik}^{\infty} - G_{ij}^{\infty}\right)$ from Eq. (10), yet, they are required for the Kirkwood-Buff inversion and the calculation of *fundamental structure making/breaking functions* $\mathscr{S}_{i\alpha}^{\infty}(T,P,x_{\alpha})$.

In Figs. 5–7, we illustrate the microstructural behavior of the ethyl acetate (j) + k-cosolvent binary systems over the entire composition range in terms of three Kirkwood-Buff integrals $G_{\alpha\beta}(x_j)$ and the two resulting fundamental structure making/breaking functions $\mathscr{S}_{\alpha\beta}(x_j)$. According to Figs. 5a–7a, the three binaries exhibit positive deviations from Lewis-Randall ideality, $\Delta_{jk}(x_j) > 0$, resulting from the $G_{jk}(0 \le x_j \le 1) < 0$ and $0.5(G_{jj} + G_{kk}) > |G_{jk}|$. Note that while methanol and ethanol show a slight enhancement of $G_{\alpha\alpha}(x_{\alpha} < 0.15)$ from their pure component values $G_{\alpha\alpha}^{o} = kT\kappa_{\alpha}^{o} - v_{\alpha}^{o}$, 2-propanol exhibits a continuous weakening of $G_{\alpha\alpha}(x_{\alpha})$. In contrast, ethyl acetate in solution (with methanol, ethanol, and 2-propanol) enhances its microstructure around itself from its pure component condition $G_{ETAC-ETAC}^{o} = kT\kappa_{ETAC-ETAC}^{o} - v_{ETAC-ETAC}^{o} < 0$, and while $G_{ETAC-ETAC}(x)$ stays negative when in solution with methanol and ethanol over all compositions, it becomes slightly positive at infinite dilution in 2-propanol, $G_{ETAC-ETAC}(x_{2-PROH} \to 1) \gtrapprox 0$.

Moreover, Figs. 5b–7b illustrate the composition dependence of the two structure making/breaking functions, where $\mathscr{S}_{ETAC\,k}(x_j)$ describes the $k-$ cosolvent effect on the *ETAC* $-$ solvent structure and $\mathscr{S}_{k\,ETAC}(x_j)$ portrays the *ETAC* $-$ solvent effect on the structure of the $k-$ cosolvent. Thus, $\mathscr{S}_{ETAC\,k}(x_j = 1) = 0$ and $\mathscr{S}_{k\,ETAC}(x_j = 0) = 0$, with $\mathscr{S}_{ETAC\,k}(x_j = 0) < 0$ and $\mathscr{S}_{k\,ETAC}(x_j = 1) > 0$ so that they exhibit a minimum $\mathscr{S}_{\alpha\beta}^{minimum}(0.5 < x_j < 0.6) < 0$. These figures also indicate that the three $k-$ cosolvents induce the breaking of the *ETAC* $-$ structure between $0 \le x_{ETAC} < x_{ETAC}^{0}$, where $\mathscr{S}_{k\,ETAC}(x_{ETAC}^{0} \ne 0) = 0$ with $x_{ETAC}^{0} \cong [0.73, 0.78, 0.88]$ for $k = [methanol, ethanol, 2-propanol]$, respectively. Then, for $x_{ETAC} > x_{ETAC}^{0}$, the three $k-$ cosolvents reverse their trend to become makers of the *ETAC* $-$ structure. In contrast, all $k-$ cosolvent exhibit the same *ETAC* $-$ structure breaking behavior, $\mathscr{S}_{ETAC\,k}(0 \le x_{ETAC} \le 1) < 0$, across the entire composition range of the mixed-solvent system. Here we must reemphasize that, as discussed in §2.1, the solvation of an $i-$ solute at infinite dilution in a mixed $(j+k)-$ solvent environment is characterized by four *fundamental structure making/breaking functions* $\mathscr{S}_{\alpha\beta}(x_j)$, two associated with the solvent-cosolvent interactions, $\mathscr{S}_{ETAC\,k}(x_j)$ and $\mathscr{S}_{k\,ETAC}(x_j)$, and the remaining linked to the interaction of the $i-$ solute with the solvent and the cosolvent (methanol, ethanol, 2-propanol) interactions, $\mathscr{S}_{i\,ETAC}^{\infty}(x_j)$ and $\mathscr{S}_{ik}^{\infty}(x_j)$. In other words, the preferential solvation behavior of any infinitely dilute $i-$ solute depends on four distinctive *fundamental structure making/breaking functions* as explicitly described by Eq. (18). Therefore, in this context the frequently found statement in the

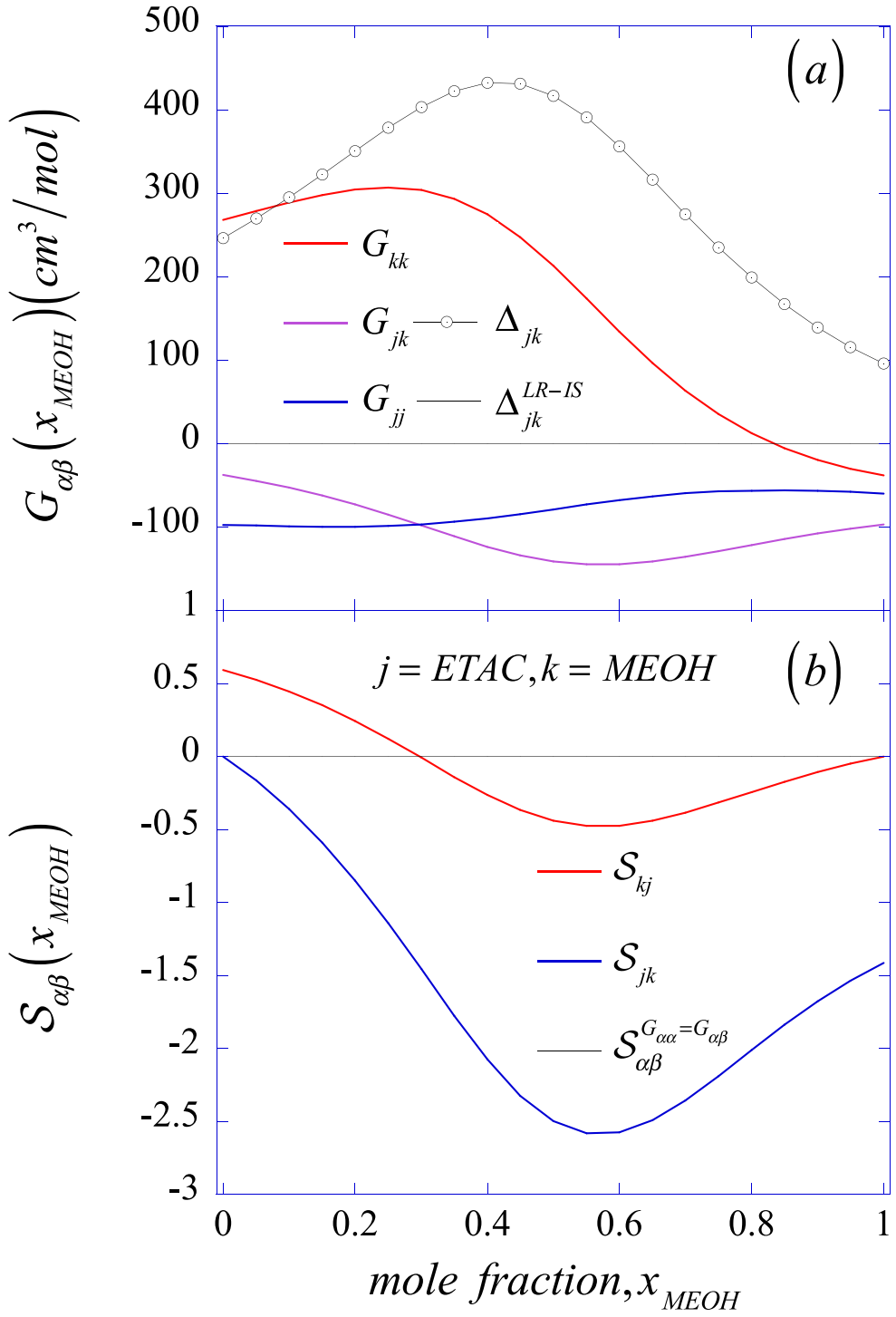

FIG. 5. Microstructural characterization of the behavior of the ethyl acetate (j) + methanol (k) binary systems in terms of the Kirkwood-Buff integrals (top) and resulting fundamental structure making/breaking functions (bottom).

literature "… *the solvent action may be related to the breaking of the slightly ordered structure of ethanol molecules…*" regarding the preferential solvation of solutes in ethyl acetate-ethanol mixed-solvent systems [79–83] becomes unsupported and misleading while providing no explicit (microscopic or otherwise) depiction of either the meaning of "*slightly ordered structure*" or the signature of the "*breaking*" event.

Furthermore, in Figure 8ab, we compare the resulting macroscopic behavior in terms of the isochoric-isothermal cosolvent (k) pressure perturbation, and its effect on their material stability with respect to their Lewis-Randall solution ideality reference counterparts. According to Fig. 8a, it becomes evident the significantly large $ETAC$ − cosolvent (k) intermolecular asymmetry, *i.e.*, $(\partial P/\partial x_{MEOH})_{T\rho_o}^{x_{ETAC}=1} \ll (\partial P/\partial x_{ETOH})_{T\rho_o}^{x_{ETAC}=1} \ll (\partial P/\partial x_{2PROH})_{T\rho_o}^{x_{ETAC}=1} \ll 0$, and similarly for the other limiting condition. This large $ETAC$ − cosolvent (k) intermolecular asymmetry, that resulted in a significant positive deviation from the Lewis-Randall ideal solution reference (see Figs. 5a–7a, $\Delta_{jk}^{LR-IS} = 0$, [84] becomes also evident in Fig. 8b, where we can observe a rather symmetric composition dependence $\mathscr{D}(x_{ETAC})$, following the trend $\mathscr{D}_{ETAC\,2-PROH}(x) > \mathscr{D}_{ETAC\,ETOH}(x) > \mathscr{D}_{ETAC\,MEOH}(x) > 0$ toward the limit of stability, $\mathscr{D}(x) =$

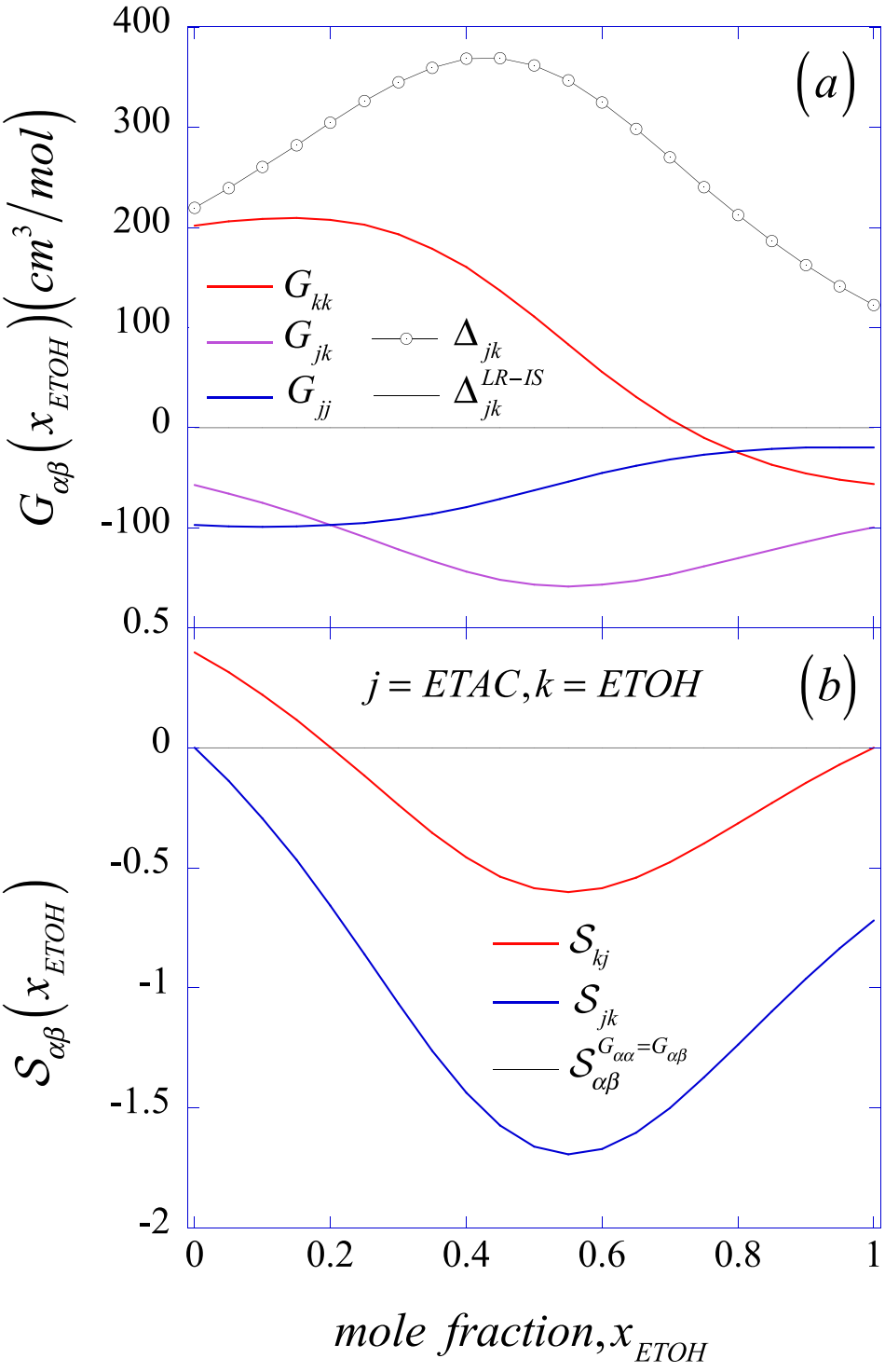

Fig. 6. Microstructural characterization of the behavior of the ethyl acetate (j) + ethanol (k) binary systems in terms of the Kirkwood-Buff integrals (top) and resulting fundamental structure making/breaking functions (bottom).

0. The depicted behavior in Figures (5)-(8), portraying the extent of the deviation from the Lewis-Randall ideal solution reference, highlights the failure of the mixed-solvent ideality assumption in the modeling of low solubility solutes, $\mathscr{D}^{LR-IS}(x_j) = 1$, especially when involving aqueous-organic mixed-solvent systems [85,86]

Now, to gain some understanding of the preferential solvation behavior of *DHEA-A* (i) in ethyl acetate (j) + cosolvent (k), we display in Figs. 9–11 the four contributing *fundamental structure making/breaking functions* $\mathscr{S}_{\alpha\beta}(x_k)$ to the *universal preferential solvation* $\mathscr{PS}(x_k)$ and the first-order preferential solvation parameter $\delta^0_{k\ DHEA-A}(x_k)$. Given that the composition behavior of $\mathscr{S}_{jk}(x_k)$ and $\mathscr{S}_{kj}(x_k)$ has been already discussed around the Figs. 5a–7a, we focus on the behavior of $\mathscr{S}^{\infty}_{DHEA-A\ k}(x_k)$in Figs. 9a–11a, where we observed that $\mathscr{S}^{\infty}_{DHEA-A\ ETAC}(x_k) \leq 0$and exhibits a minimum around $0.6 < x_k < 0.7$ for $k = (MEOH, ETOH)$, Figs. 9a, 10a, while it becomes rather flat with inflexions for $k = 2PROH$, Fig. 11a. In contrast, $\mathscr{S}^{\infty}_{DHEA-A\ k}(x_k) \leq 0$ and exhibits a minimum and a maximum around $0.6 < x_k < 0.7$ for $k = (MEOH, ETOH)$, Figs. 9a, 10a, a feature that transforms to an inflexion for $k = 2PROH$in Fig. 11a. Moreover,

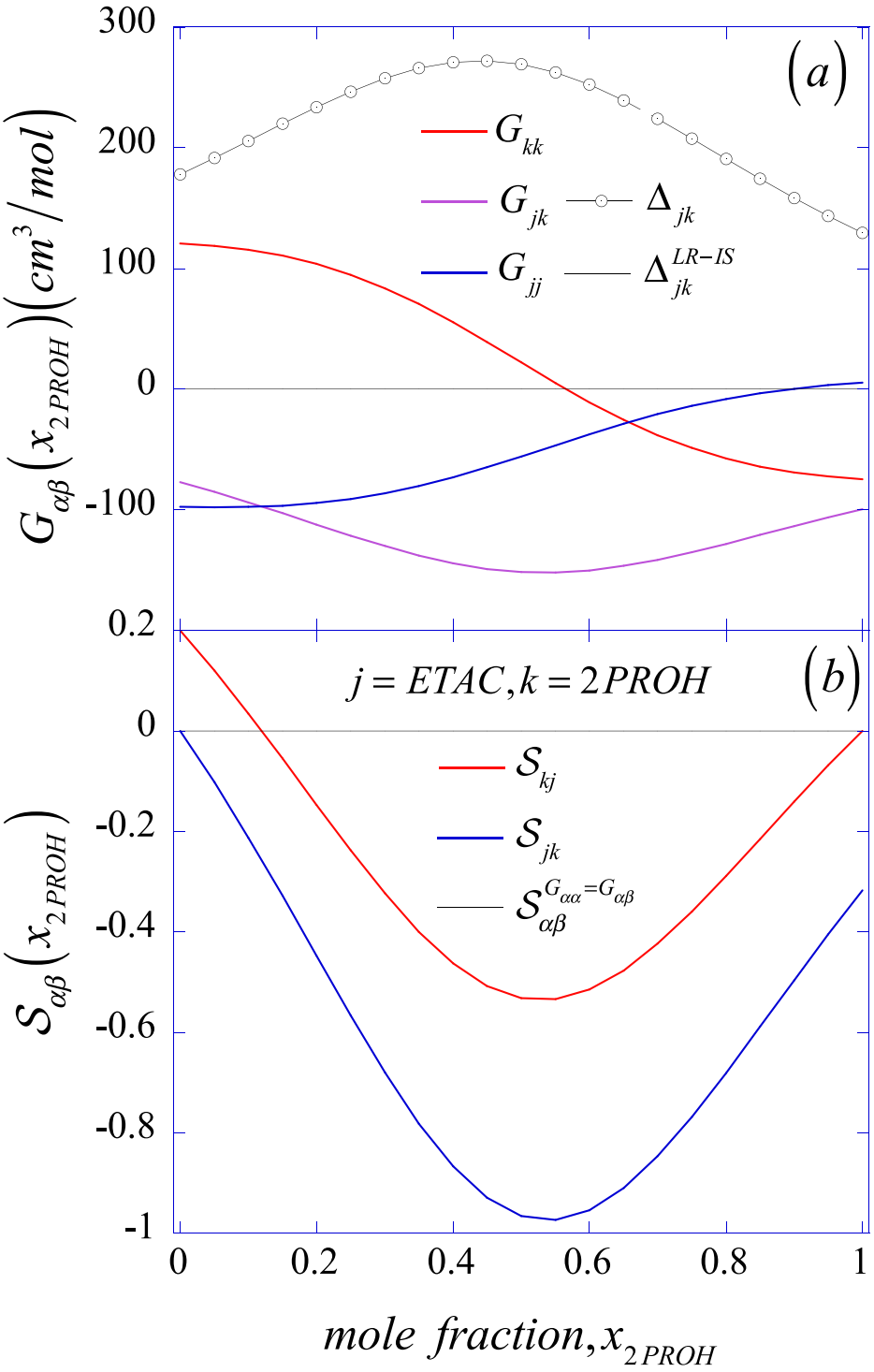

Fig. 7. Microstructural characterization of the behavior of the ethyl acetate (*j*) + 2-propanol (*k*) binary systems in terms of the Kirkwood-Buff integrals (top) and resulting fundamental structure making/breaking functions (bottom).

according to Figs. 9b–11b, the *universal preferential solvation* $\mathscr{PS}(x_k)$ of *DHEA-A* (*i*) in the three cosolvents (*k*) exhibit similar behavior, *i.e.*, two peaks (or a shoulder and a peak for ethanol as cosolvent) around $x_k = 0.2$ and $x_k = 0.8$. Note also that the corresponding first order preferential solvation parameters, $-\delta^0_{k\,DHEA-A}(x_k)$ in Figs. 9b–11b, follow similar composition trends with obviously the $\delta^0_{k\,DHEA-A}(x_k = 0) = \delta^0_{k\,DHEA-A}(x_k = 1) = 0$ limiting behavior by definition. This limiting behavior is precisely the major shortcoming of $\delta^0_{ik}(x_k)$ as marker of preferential solvation phenomena given that it describes an identical behavior for all systems regardless of either their solute-solvent or solute-cosolvent intermolecular interactions asymmetries [32,37].

4.2. *Illustration of the preferential solvation of a few representative pharmaceutical solutes in a common organic mixed-solvent environment*

In this case, we analyze the preferential solvation behavior of a few pharmaceutical solutes in a common mixed ethyl acetate (*j*) + ethyl alcohol (*k*) environment. For this purpose, we chose the following six *i* –

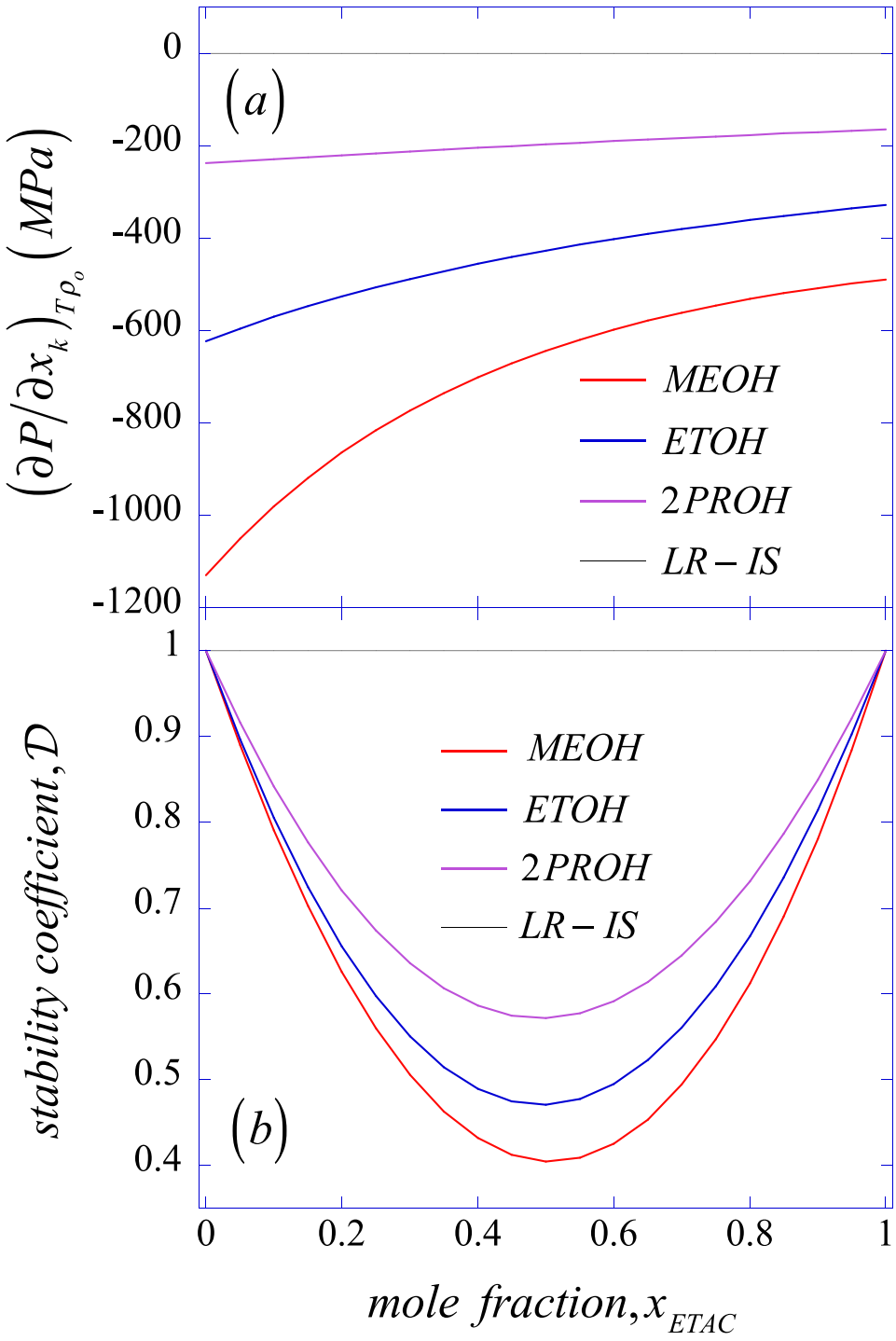

Fig. 8. Comparison of the behavior of the three mixed-solvent systems in terms of the isochoric-isothermal $k-$ cosolvent pressure perturbation (top), and its effect on their material stability with respect to their Lewis-Randall solution ideality reference counterparts (bottom).

solutes for which we have solubility data along the $T = 313K$ isotherm under ambient pressure: indomethacin, [79] naproxen, [79] meloxicam, [80] and piroxicam, [81] used as nonsteroidal anti-inflammatory drugs, while mevastatin, [82] prescribed as cholesterol-lowering agent, and posaconazole, [83] involved in the treatment of fungal infections [87].

In Figure 12ab, we compare the *universal preferential solvation* $\mathscr{PS}(x_{ETAC})$ behavior of six pharmaceutical solutes in ethyl acetate-ethanol mixed-solvent systems (top part) and contrast them with the corresponding first-order preferential solvation parameter $\delta^0_{ETAC\,i}(x_{ETAC})$ (bottom part). The outstanding feature of the observed $\mathscr{PS}(x_{ETAC})$ behavior is their increasing trend with increasing x_{ETAC}, except for posaconazole that shows a significant increase up to $x_{ETAC} \simeq 0.6$, and then a decrease to slightly negative, when reaches the condition of pure ethyl acetate. In other words, the fact that $\mathscr{PS}(x_{ETAC} < x^0) < 0$ in Fig. 12a indicates that these pharmaceutical solutes prefer ethyl acetate as a solvation environment over ethanol within the highlighted composition range, while microscopically manifested as $G^{\infty}_{i\,ETAC}(x_{ETAC} < x^0) > G^{\infty}_{i\,ETOH}(x_{ETAC} < x^0)$ or macroscopically as $\mathscr{PS}(x_{ETAC} < x^0) < 0$, $\Delta_{tr}g_i(0 < x_{ETAC} < x^0) < 0$, $\left[\partial \Delta_{tr}g_i(x_{ETAC} < x^0)/\partial x_{ETAC}\right]_{TP} < 0$ and $\left[\partial \mu^{\ominus}_i(x_{ETAC})/\partial \mu_{ETAC}(x_{ETAC})\right]_{TP} < 0$, where x^0 the composition of the

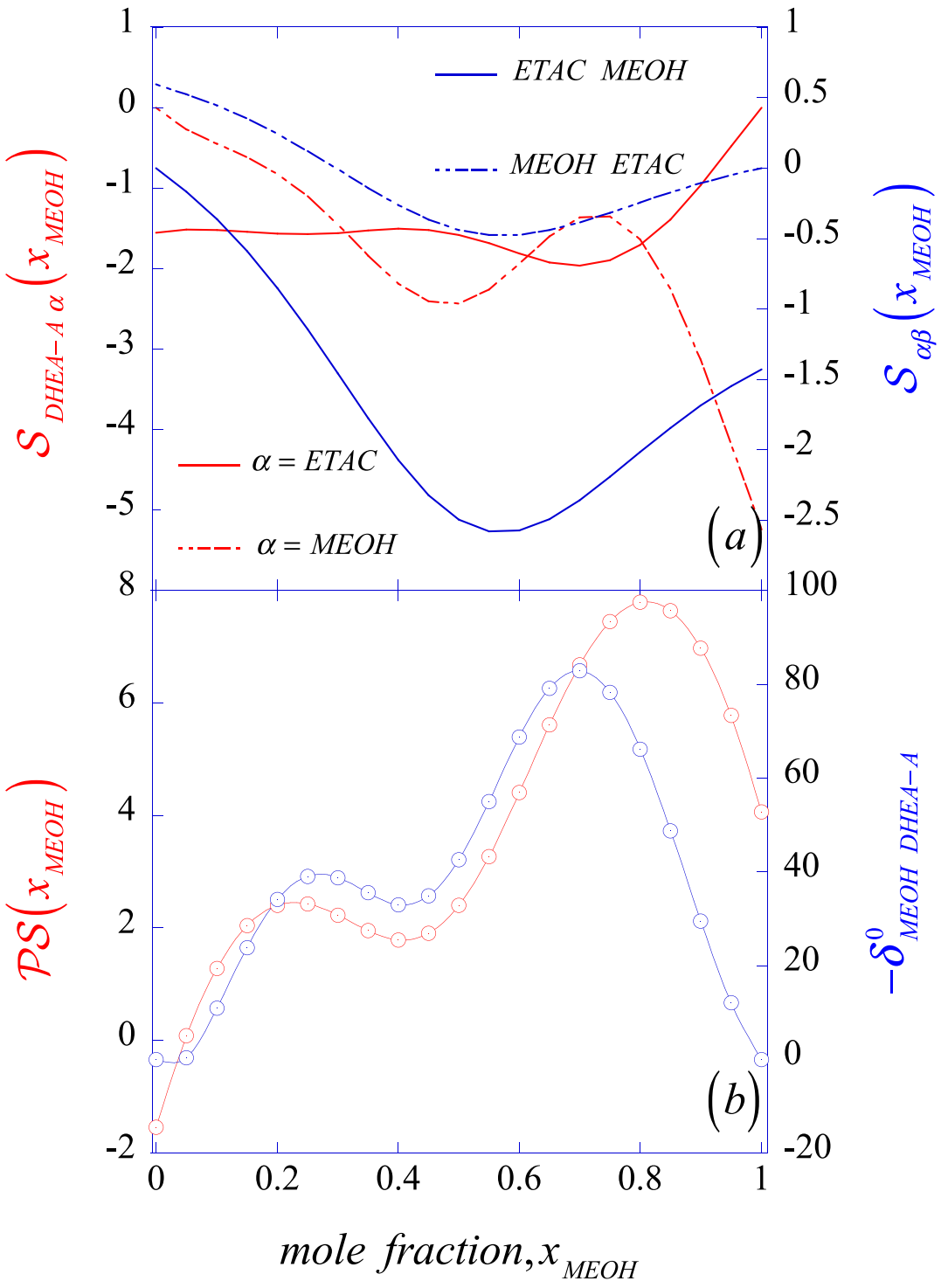

Fig. 9. Color-coordinated solvation behavior of *DHEA-A* (*i*) in ethyl acetate (*j*) + methanol (*k*) in terms of the four *fundamental structure making/breaking functions* $\mathscr{S}_{\alpha\beta}(x_k)$ contributions (top), and the resulting *universal preferential solvation* $\mathscr{PS}(x_k)$ as well as the first-order preferential solvation parameter $\delta^0_{k\ DHEA-A}(x_k)$ as a function of the methanol bulk composition at ambient conditions.

mixed-solvent at which the $i-$ solute prefers the two solvents equally, *i.e.*, $\mathscr{PS}\left(x_{ETAC}=x^0\right)=0$. Note however that the observed increasing trend of $\mathscr{PS}(x_{ETAC})$ is not monotonous in mixed-solvent composition, in that it exhibits either inflexion points (*e.g.*, piroxicam and meloxican) or relative extrema (*e.g.*, mevastatin and posaconazole).

In contrast to the behavior of $\mathscr{PS}(x_{ETAC})$, and due to its formal definition, the corresponding $\delta^0_{ETAC\ i}(x_{ETAC})$ exhibit always a wavy shape and comprise three roots, i.e., $\delta^0_{ETAC\ i}(x_{ETAC})=0$ for $\{x_{ETAC}=0; x_{ETAC}=1; 0<x_{ETAC}<1\}$. This behavior highlights precisely the main drawback behind the use of $\delta^0_{ETAC\ i}(x_{ETAC})$ as a marker for preferential solvation as extensively discussed elsewhere [32]. Moreover, as a matter of illustration in Fig. 13a, b, we compare $\rho_o\delta^{0,faulty}_{ji}=x_jx_k\rho_o\left(G^{\infty,faulty}_{ij}-G^{\infty}_{ik}\right)$, *i.e.*, from using the incorrectly inverted Kirkwood-Buff integrals, *e.g.*, Eqs. (26)–(30) in §3.2, against the intended $\rho_o\delta^0_{ji}\equiv x_jx_k\rho_o\left(G^{\infty}_{ij}-G^{\infty}_{ik}\right)$ for the same set of systems in Fig. 12. Not surprisingly, the contrasting behavior

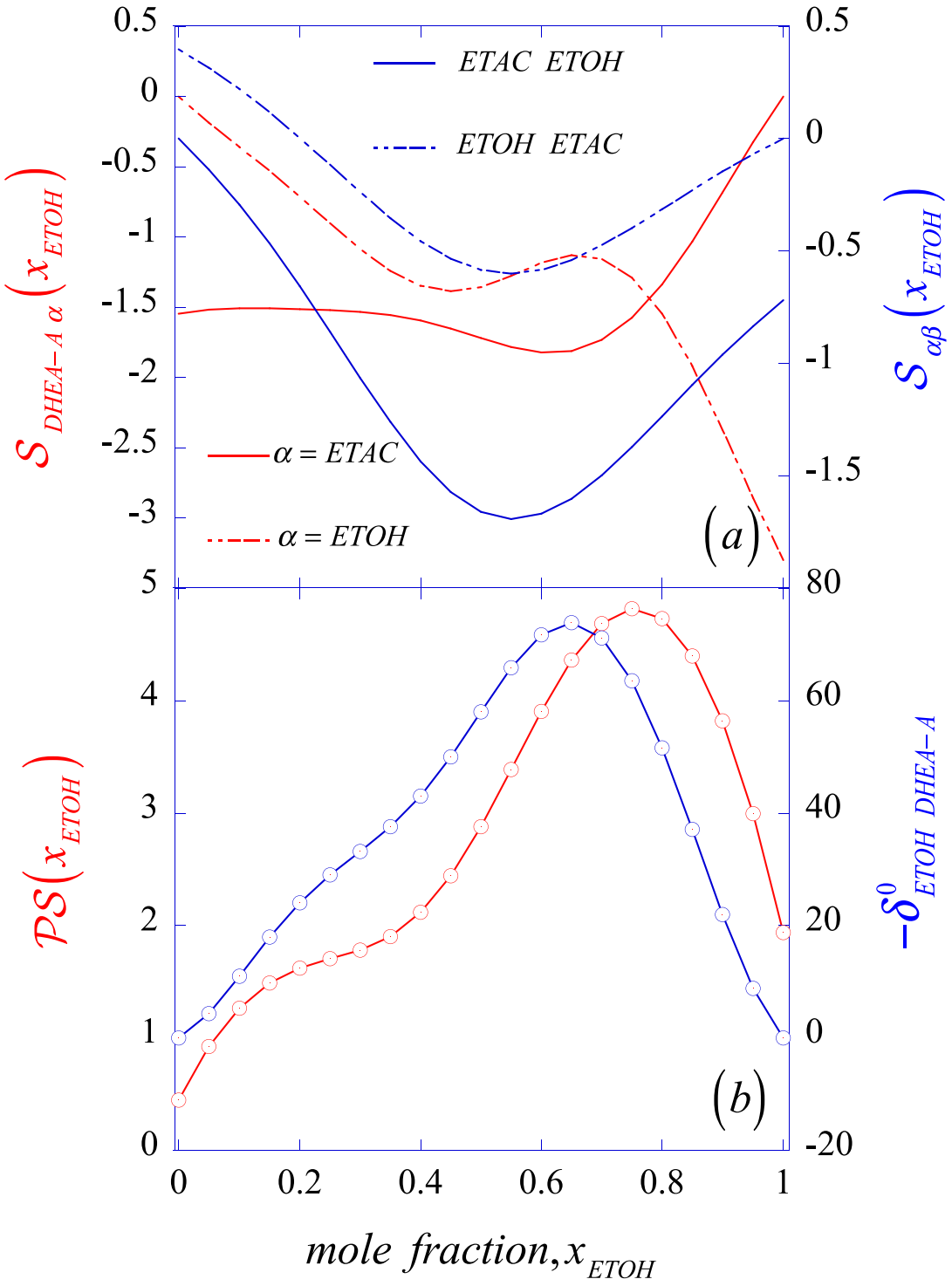

Fig. 10. Color-coordinated solvation behavior of *DHEA-A* (i) in ethyl acetate (j) + ethanol (k) in terms of the four *fundamental structure making/breaking functions* $\mathscr{S}_{\alpha\beta}(x_k)$ contributions (top), and the resulting *universal preferential solvation* $\mathscr{PS}(x_k)$ as well as the first-order preferential solvation parameter $\delta^0_{k\ DHEA-A}(x_k)$ as a function of the ethanol bulk composition at ambient conditions.

between $\rho_o\delta^0_{ETAC\ i}(x_{ETAC})$ and $\rho_o\delta^{0,faulty}_{ETAC\ i}(x_{ETAC})$ becomes immediately obvious in Fig. 13a, b: $\rho_o\delta^0_{ETAC\ i}(x_{ETAC}<0.37)>0$ in comparison with $\rho_o\delta^{0,faulty}_{ETAC\ i}(x_{ETAC}<0.37)<0$, where $x_{ETAC}\cong 0.37$ is the common middle root of $\delta^{0,faulty}_{ETAC\ i}(x_{ETAC})=0$ regardless of the identity of the $i-$ solute. This common middle root of $\delta^{0,faulty}_{ji}(x_j)=0$ for any solute in the same mixed-solvent system results from the solution of A8 in Appendix A. Moreover, we can clearly confirm in Fig. 13a, b that $\delta^{faulty}_{ji}(x_j\to 1)\to\delta_{ji}(x_j)$, as expected from the expressions A1–A6 in the Appendix A.

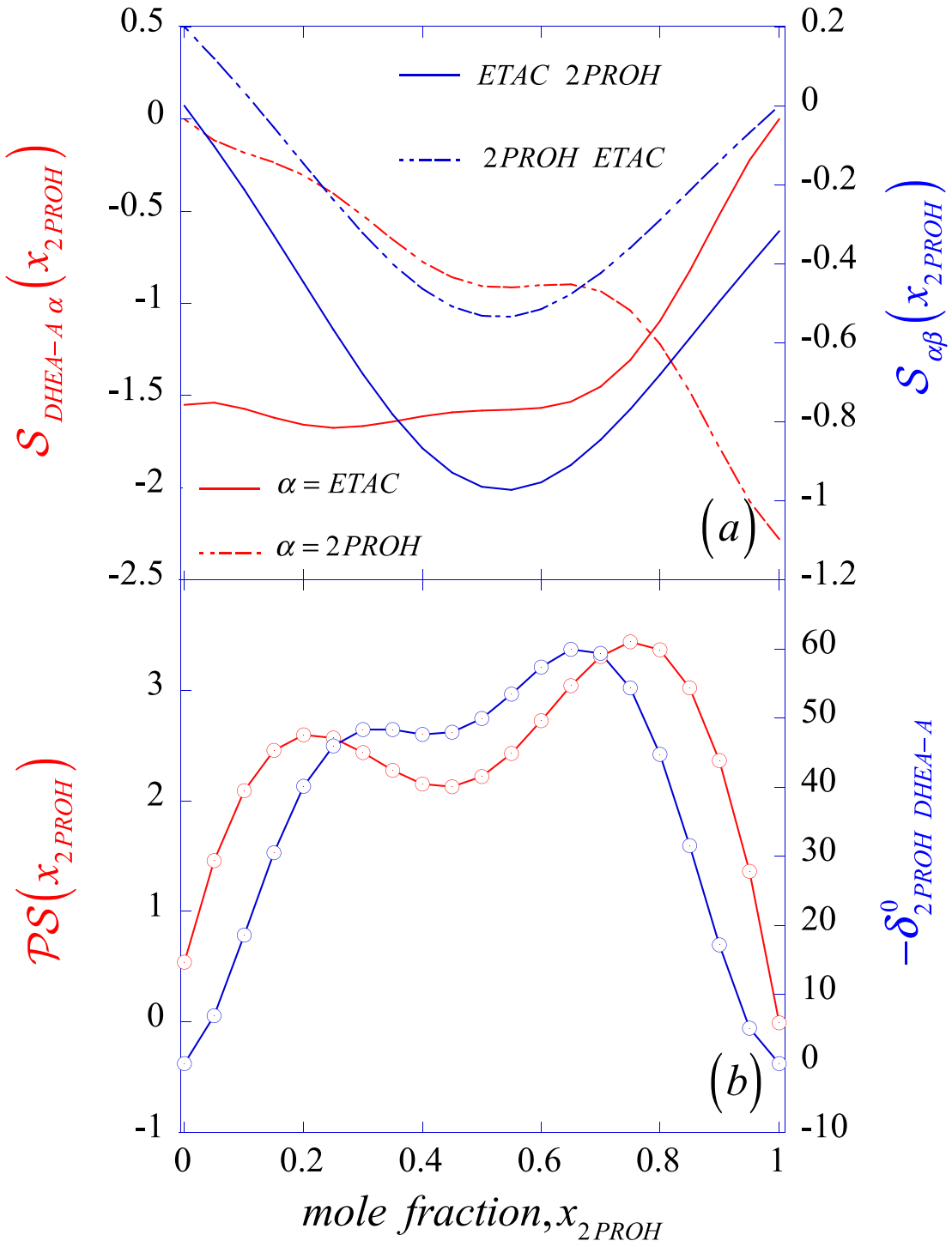

Fig. 11. Color-coordinated solvation behavior of *DHEA-A* (*i*) in ethyl acetate (*j*) + 2-propanol (*k*) in terms of the four *fundamental structure making/breaking functions* $\mathscr{S}_{\alpha\beta}(x_k)$ contributions (top), and the resulting *universal preferential solvation* $\mathscr{PS}(x_k)$ as well as the first-order preferential solvation parameter $\delta^0_{k\ DHEA-A}(x_k)$ as a function of the isopropanol bulk composition at ambient conditions.

5. Discussion, observations and recommendations

The relevant issue we must emphasize, regardless of the choice of modeling scheme for the solvent effects, is how the resulting approach can guide the selection of cosolvents for any specific application under consideration, *e.g.*, to improve separation, enhance solubility, and control transport properties through the manipulation of the mixed-solvent environment. We frequently encounter studies whose sole outcome is a composition profile of a preferential solvation marker leading usually to handwaving interpretations about either the interplays of solute-solvent/solute-cosolvent and solvent-cosolvent interactions or unsupported conjectured structure making/breaking events. Although these studies usually involve significant experimental effort associated with the solubility measurements and data regression, unfortunately, their value is undermined by the absence of any explicit connections between the mixed-solvent composition, the preferential solvation markers, and the actual system microstructure. In other words, these studies usually provide handwaving arguments and unsupported conjectures, while the

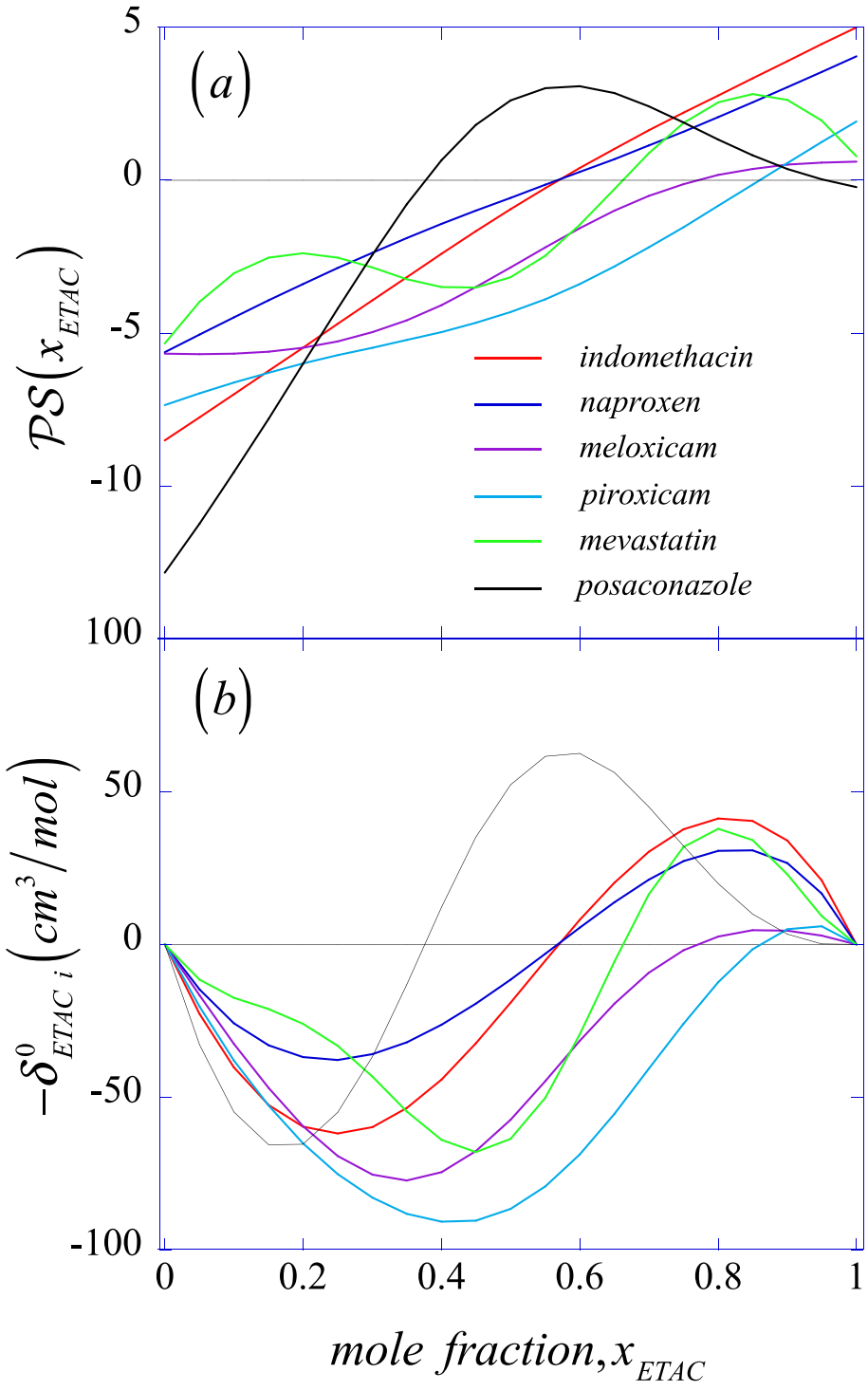

Fig. 12. Preferential solvation behavior of six pharmaceutical solutes in a common mixed ethyl acetate (j) + ethanol (k) environment described by the *universal preferential solvation* $\mathcal{PS}(x_{ETAC})$ (top), and the corresponding first-order preferential solvation parameter $-\delta^0_{ETAC\ i}(x_{ETAC})$ (bottom) along the $T = 313K$ isotherm under ambient pressure.

readers are left with no means to link (and consequently manipulate) the measured solvent effect either with any thermodynamic *preferential solvation interaction parameter* [88,89] or rate of change of the solute standard chemical potential upon changes in the mixed-solvent composition, usually measured in terms of Gibbs free energy of transfer [32]

In contrast to the discussed deficiencies in current approaches, we have proposed an alternative rigorous solvation formalism comprising *fundamental structure making/breaking functions* leading to a rigorous *preferential solvation* framework. This alternative allows the unraveling of the unambiguous cause-effect connections between the solute-induced differential microstructural perturbation of the mixed-solvent environment, *aka* the preferential solvation, and its macroscopic response, described by a unique *thermodynamic preferential interaction parameter*. Note that, the thermodynamic *preferential solvation interaction parameters* for an $i-$ solute involving $j-$ and $k-$ diffusible species in

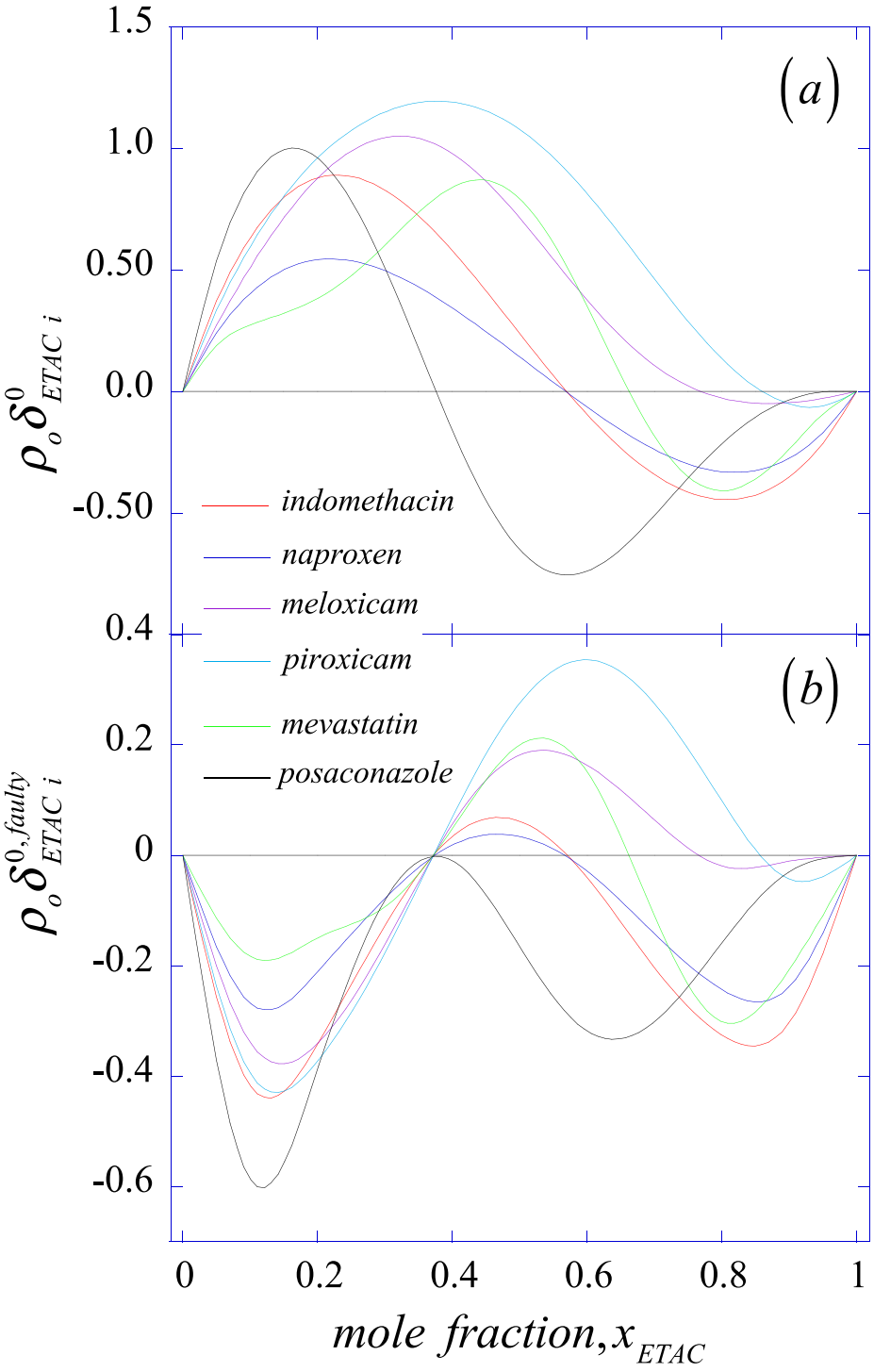

Fig. 13. Preferential solvation behavior of six pharmaceutical solutes in a common mixed ethyl acetate (j) + ethanol (k) environment described by the dimensionless first-order preferential solvation parameter $\rho_o \delta^0_{ETAC\ i}(x_{ETAC})$ (top), and the corresponding $\rho_o \delta^{0,faulty}_{ETAC\ i}(x_{ETAC})$ (bottom) along the $T = 313K$ isotherm under ambient pressure.

open and semi-open systems, leading to $\Gamma^{(\chi_i)}_{\mu_j\mu_k}(x_j) = (\partial\chi_k/\partial\chi_i)_{T\mu_j\mu_k}$ and $\Gamma^{(\chi_i)}_{\mu_\alpha}(x_j) = (\partial\chi_k/\partial\chi_i)_{TP\mu_\alpha}$ for $\chi = (\rho, m, x)$ with $\alpha = (j, k)$, have been rigorously characterized in terms of Kirkwood-Buff integrals [29] and *fundamental structure making/breaking functions* [32] However, only one of them actually describes the *universal preferential solvation* $\mathscr{PS}(x_j) = \rho_o\left(G^{\infty}_{ik} - G^{\infty}_{ij}\right)$, as discussed extensively elsewhere [32,37]. In fact, since $\Gamma^{(x_i\to 0)}_{ik}(x_j) = \Gamma^{(m_i\to 0)}_{\mu_j\mu_k}(x_j) \equiv (\partial m_k/\partial m_i)_{T\mu_j\mu_k}$ with $\Gamma^{(x_i\to 0)}_{ik}(x_j) = x_k\mathscr{PS}(x_j)$, we can now make a unique unambiguous connection between the thermodynamic response of the solute standard chemical potential, (or its corresponding Gibbs free energy of transfer) upon changes in the mixed-solvent composition, and the microstructural perturbations experinced by the solvent environment around the solute. This explicit microscopic-to-macroscopic link captures the fundamental notion underlying the thermodynamic solvent effect and its applications in chemical/separation processes, and highlights one of the main shortcomings in existing studies of preferential solvation.

In fact, the alluded missing link in current studies prevents revealing how the preferential solvation parameters (or any relative affinity marker for that matter) might be quantitatively applied to manipulate and tune the mixed-solvent environment for the different purposes behind the use of these environments in the first place. Instead, what we often encountered are unsupported interpretations of the composition dependence of a particular preferential solvation marker according to likely mechanisms of intermolecular interactions [66,90–93]. Moreover, practitioners of molecular modeling are frequently confronted with unexpected outcomes which usually lead to the search for interpretations and plausible explanations of the observations rather than trying first to assess the validity of the involved formalism or the correctness of the underlying calculations [94–96]. This is specially the case when following *black box* approaches, resulting from the use of packaged routines (*e.g.*, EoS involving conjectured mixing rules) or the direct application of published formalisms without verifying their correctness, *e.g.*, the local composition approach to preferential solvation as discussed in §3.1–3.3.

In the context of the previously described scenario, the proposed unambiguous preferential solvation formalism has afforded us the tools to (*a*) study the actual preferential solvation behavior of pharmaceuticals (or any other species for that matter) in mixed-solvents, (*b*) offered a rigorous interpretation of the differential affinity between the solute and the components of the solvent environment in terms of the *fundamental structure making/breaking functions*, and (*c*) assessed the ability of a frequently used local composition model to describe solvent effects, as well as test the self-consistency and correctness of its underlying equations. Moreover, the critical analysis of the methods and forensics of the published data have underscored some useful observations about their foundations, implementation, and limitations, including:

(*i*) The straightforward determination of the corresponding correlation radius $R_c(x_j) = \sqrt[3]{3V_c/4\pi}$ from the iterated $V_c\left(\widehat{v}^{\infty}_i, x^{L}_{ji}, x_j\right)$ usually confirms that the resulting $R_c(x_j)$ values are usually rather small, *i.e.*, $R_c(x_j) < 10$Å. Consequently, the requirement $G_{ij}(R_c) \cong -V_c$ underlying Eq. (25) or its alternative $g_{ij}(r \geq R_c) \cong 1$ might not be fulfilled at all. In fact, this requirement translates into $G_{ij}(R_c > \zeta) \cong -V_c < -4\pi\zeta^3/3$ where ζ is the correlation length of the fluid environment so that $g_{ij}(r \geq \zeta) \cong 1$. According to the molecular simulations of water at ambient conditions, $\zeta \geq 15$Å, [58, 59] *i.e.*, validating the concern;

(*ii*) Because $\delta_{ji}(x_j)$ represents a rational expression whose denominator must be positive at any composition for a stable homogeneous phase, while the numerator exhibits a continuous dependence with the mixed-solvent composition, *i.e.*,

$$\begin{aligned}\delta_{ji}(R_c) &= x_j x_k\left(G^{\infty}_{ij} - G^{\infty}_{ik}\right)\Big/\left(x_j G^{\infty}_{ij} + x_k G^{\infty}_{ik} + V_c\right)\\ &= x_j x_k\mathscr{PS}\Big/\left(\rho_j G^{\infty}_{ij} + \rho_k G^{\infty}_{ik} + V_c V^{-1}\right)\\ &= x_j x_k\left[\partial\Delta_{tr}g_i(x_j)/\partial x_j\right]_{TP}\Big/\left[kT\mathscr{D}\left(\rho_j G^{\infty}_{ij} + \rho_k G^{\infty}_{ik} + V_c V^{-1}\right)\right]\end{aligned} \tag{42}$$

any discontinuous behavior in the processed experimental data through Eq. (24) is an early sign of something clearly wrong with the implementation of the formalism;

(*iii*) In addition to implementing a *correct* formalism, the invoked approximations should always be thermodynamically consistent, including the representations of $\widehat{v}^{\infty}_i(T,P,x_j)$ and $\kappa_o(T,P,x_j)$, where the excess properties $\mathscr{P}^E(T,P,x_j)$ must obey $\mathscr{P}^E(T,P,x_j=1) = 0$ and $\mathscr{P}^E(T,P,x_j=0) = 0$ requirements. These two issues are often unfulfilled in the cited literature, where the regressed $g^E(T,P,x_j)$ describing $g^E(x_j = 0 \text{ and/or } x_j = 1) \neq 0$, [79,97–102] not only does it represent an obvious thermodynamic inconsistency, but also does it corrupt the resulting composition profiles of the solvent-cosolvent intermolecular interaction asymmetry embodied by $\Delta_{jk}(T,P,x_j)$. In turn, this could result in an ill-behaved coefficient of material stability $\mathscr{D}(T,P,x_j)$;

(iv) The assumption of Lewis-Randall ideal solution for the behavior of the mixed-solvent in the modeling of low-solubility pharmaceutical solutes introduces unnecessary inaccuracies to the description of the mixed-solvent, [85,86] and leads to additional microstructural and thermodynamic inaccuracies in the analysis of the relevant preferential solvation target, to compensate for the non-ideal solute-solvent and solute-cosolvent contributions.

(v) There is a need for accurate experimental data of $\widehat{v}^{\infty}_i(x_j = 0)$ and $\widehat{v}^{\infty}_i(x_j = 1)$ to either avoid the use, or test the validity, of the conjectured $\widehat{v}^{\infty}_i(x_j) \cong v^o_i$ especially after considering that $\widehat{v}^{\infty}_i(x_j) \cong v^o_i$, in contrast to $\kappa_o(x_j)$, has a similar magnitude to that of the resulting $G^{\infty}_{i\alpha}(x_j)$, i.e., Eqs. (11), (12), and;

(vi) The direct calculation of the $\mathscr{PS}$, Eq. (10), does not require data of either $\kappa_o(x_j)$ or $\widehat{v}^{\infty}_i(x_j)$ in contrast to the determination of $\delta_{ji}(R_c)$ which needs the full proper inversion of the Kirkwood-Buff formalism. This is an important issue considering that both properties are scarcely available experimentally, and usually require the use of approximations as we discussed below.

We should note that, to overcome the lack of data for $\widehat{v}^{\infty}_i(T,P,x_j)$ and $\kappa_o(T,P,x_j)$, we usually invoke Krichevskii's ideality [103] for the $i-$solute in the mixed-solvent system and Lewis-Randall's ideality for the isothermal compressibility of the binary mixed-solvent environment [69]. The first ideality condition can be written in terms of fugacity

coefficients as follows, [32,37].

$$\ln\widehat{\phi}^{\infty}_{i,j+k}(T,P,x_j) \cong x_j \ln\widehat{\phi}^{\infty}_{i,j} + (1-x_j)\ln\widehat{\phi}^{\infty}_{i,k} \tag{43}$$

whose isothermal-pressure derivative (assuming that Eq. (43) holds within a finite $(P \pm \Delta P)-$ range finally) leads to the sought expression for $\widehat{v}^{\infty}_{ij+k}(T,P,x_j)$

$$\widehat{v}^{\infty}_{i,j+k}(T,P,x_j) \cong x_j \widehat{v}^{\infty}_{ij}(T,P) + (1-x_j)\widehat{v}^{\infty}_{i,k}(T,P) \tag{44}$$

where $\widehat{v}^{\infty}_{i,\alpha}(T,P)$ denotes the partial molar volume of the $i-$ solute at infinite dilution in a pure $\alpha-$ solvent at the indicated (T,P) state conditions. Unfortunately, $\widehat{v}^{\infty}_{i,\alpha}(T,P)$ of pharmaceutical species are usually not measured but approximated by the corresponding molar volume of the pure species $v^{o}_{i}(T,P)$, *e.g.*, Ref. [61] and the related publications based on this citation. Moreover, in terms of Krichevskii's ideality, the latter approximation implies the assumption $\left(\partial\ln\widehat{\phi}^{\infty}_{i,\alpha}/\partial P\right)_{Tx_\alpha} \simeq \left(\partial\ln\phi^{o}_{i}/\partial P\right)_{Tx_\alpha}$ leading to $\widehat{v}^{\infty}_{i,\alpha} \simeq v^{o}_{i}$ for $\alpha = (j,k)$, which can only be an accurate approximation if the corresponding standard partial molar volume of solute transfer, $\Delta_{tr}\widehat{v}^{\ominus}_{i}(T,P,x_j)$, is negligible small over the entire range of mixed-solvent composition, i.e.,

$$\begin{aligned}
\Delta_{tr}\widehat{v}^{\ominus}_{i}(T,P,x_j) &= \int_0^{x_j} \left(\partial\widehat{v}^{\ominus}_{i}/\partial x_j\right)_{TP} dx_j \\
&= \widehat{v}^{\ominus}_{ij+k}(T,P,x_j) - \widehat{v}^{\ominus}_{ij}(T,P,x_j=0) \\
&= \widehat{v}^{\infty}_{ij+k}(T,P,x_j) - \widehat{v}^{\infty}_{ij}(T,P,x_j=0) - \\
&\quad kT\left[\kappa_o(T,P,x_j) - \kappa_o(T,P,x_j=0)\right] \\
&= \widehat{v}^{\infty}_{ij+k}(T,P,x_j) - \widehat{v}^{\infty,IG-i}_{ij+k}(T,P,x_j) - \\
&\left[\widehat{v}^{\infty}_{ij}(T,P,x_j=0) - \widehat{v}^{\infty,IG-i}_{ij}(T,P,x_j=0)\right]
\end{aligned} \tag{45}$$

with $\widehat{v}^{\ominus}_{i}(T,P,x_j) \equiv \left(\partial\mu^{\ominus}_{i}/\partial P\right)_{Tx} = \widehat{v}^{\infty}_{i}(T,P,x_j) - kT\kappa_o(T,P,x_j)$, [104] where the last line becomes negligible small as indicated below in Eq. (48). Meanwhile, the second ideality coefficient leads to the following approximation,

$$\kappa_o(T,P,x_j) \cong x_j\left(v^{o}_{j} \Big/ v^{LR-IS}_{o}\right)\kappa^{o}_{j} + (1-x_j)\left(v^{o}_{k}/v^{LR-IS}_{o}\right)\kappa^{o}_{k} \tag{46}$$

with $v^{LR-IS}_{o} = x_j v^{o}_{j} + x_k v^{o}_{k}$ [69,70]. Frequently, [61] and publications based on Ref. [61], invoke instead the following expression,

$$\kappa_o(T,P,x_j) \cong x_j\kappa^{o}_{j} + (1-x_j)\kappa^{o}_{k} \tag{47}$$

which obviously becomes an acceptable approximation to Eq. (46) only when $v^{o}_{j}(T,P) \cong v^{o}_{k}(T,P)$. Note that under the $v^{o}_{j} \cong v^{o}_{k}$ condition, we also find that $\kappa^{o}_{j}(T,P) \cong \kappa^{o}_{k}(T,P)$ and consequently, Eqs. (45), (46) lead to the following expression for the partial molar volume of solute transfer,

$$\begin{aligned}
\Delta_{tr}\widehat{v}^{\ominus}_{i}(T,P,x_j) &= \widehat{v}^{\infty}_{ij+k}(T,P,x_j) - \widehat{v}^{\infty}_{ij}(T,P,x_j=0) - kT\left(\kappa^{o}_{k} - \kappa^{o}_{j}\right)_{TP} \\
&\cong \widehat{v}^{\infty}_{ij+k}(T,P,x_j) - \widehat{v}^{\infty}_{ij}(T,P,x_j=0)
\end{aligned} \tag{48}$$

In summary, the discussions in the previous sections carry a cautionary note, i.e., while scientific publications are in principle proofread, there are always chances of misprints, missing and wrong terms or symbols that might corrupt the validity of the resulting formalism.[1] Therefore, an enlightening way that might help understand the origin of any formal expression in a publication entails the step-by-step derivation prior to its application, a practice that also allows the validation of used approximations, the understanding of potential limitations, and the detection of other subtle problems.

CRediT authorship contribution statement

Ariel A. Chialvo: Writing – review & editing, Writing – original draft, Methodology, Investigation, Formal analysis, Data curation, Conceptualization.

Declaration of competing interest

The authors declare that they have no known competing financial interests or personal relationships that could have appeared to influence the work reported in this paper.

Data availability

All data are from the cired references.

Acknowledgments

The author expresses his gratitude to Dr. Olesya Bondarenko for her kindness in translating the original Russian version of the Ref. [103].

Supplementary materials

Supplementary material associated with this article can be found, in the online version, at doi:10.1016/j.fluid.2024.114212.

Appendix A: Relation between $\delta^{faulty}_{\alpha i}(x_\alpha)$ and $\delta_{\alpha i}(x_\alpha)$ preferential solvation parameters

Starting with Eq. (26) as the misrepresented (faulty) definition of the Kirkwood-Buff integral G^{∞}_{ij}, we immediately find that,

$$\left(G^{\infty,faulty}_{ij} \Big/ G^{\infty}_{ij}\right) = 1 + \left(2x_k\widehat{v}_k \Big/ G^{\infty}_{ij}\mathscr{D}\right)\left[\partial\ln(\widehat{\phi}_i z)^{\infty}/\partial x_j\right]_{TP} \tag{A1}$$

where $\mathscr{D} = \left[1 + \left(\partial\ln\gamma_j/\partial\ln x_j\right)_{TP}\right]$. Then, after invoking Eq. (11) for the correct inversion of G^{∞}_{ij} and the working Eq. (10), we obtain the following expression,

[1] For example, the coefficients of Eq. (56) in our previous work [37] A.A. Chialvo, O.D. Crisalle, Gas Solubility and Preferential Solvation Phenomena in Mixed-Solvents; Rigorous relations between microscopic behavior, solvation properties, and solution non-ideality, Fluid Phase Equilib., 581 (2024) 114081. were typeset incorrectly, i.e., they should actually read as $G^{E}_{ACN+H_2O}(kJ/mol) = x_{ACN}(1-x_{ACN})\left[5253 - 639(1-2x_{ACN}) + 1316(1-2x_{ACN})^2\right]$

$$\begin{aligned}\left[\partial \ln(\widehat{\phi}_i z)^{\infty}/\partial x_j\right]_{TP} &= \rho_o \mathscr{D}\left[\left(G_{ik}^{\infty} - G_{ij}^{\infty,faulty}\right) + \left(G_{ij}^{\infty,faulty} - G_{ij}^{\infty}\right)\right] \\ &= \rho_o \mathscr{D}\left(G_{ik}^{\infty} - G_{ij}^{\infty,faulty}\right) + 2\rho_o x_k \widehat{v}_k \left[\partial \ln(\widehat{\phi}_i z)^{\infty}/\partial x_j\right]_{TP}\end{aligned} \tag{A2}$$

which after invoking the identity $\rho_o^{-1} = x_k\widehat{v}_k + x_j\widehat{v}_j$ straightforward manipulations reduces to,

$$\left(G_{ij}^{\infty,faulty} - G_{ik}^{\infty}\right) = \mathscr{D}^{-1}\left[\partial \ln(\widehat{\phi}_i z)^{\infty}/\partial x_j\right]_{TP}\left(x_k\widehat{v}_k - x_j\widehat{v}_j\right) \tag{A3}$$

For any given mixed-solvent system for which we have its thermodynamic properties, *i.e.*, the input for the preferential solvation analysis, A3 provides the magnitude of the deviation of $G_{ij}^{\infty,faulty}$ from the correct value.

Now, from the definition of $\delta_{\alpha i}(x_\alpha)$, Eq. (24), and after invoking A2-A3, we have that

$$\delta_{ji}(x_j) = \frac{\delta_{ji}^{faulty}(x_j)\left(x_j G_{ij}^{\infty,faulty} + x_k G_{ik}^{\infty} + V_c^{faulty}\right) - 2x_j x_k^2 \widehat{v}_k \mathscr{D}^{-1}\left[\partial \ln(\widehat{\phi}_i z)^{\infty}/\partial x_j\right]_{TP}}{\left(x_j G_{ij}^{\infty} + x_k G_{ik}^{\infty} + V_c\right)} \tag{A4}$$

and thus,

$$\delta_{ji}^{faulty}(x_j) = \frac{\delta_{ji}(x_j)\left(x_j G_{ij}^{\infty} + x_k G_{ik}^{\infty} + V_c\right) + 2x_j x_k^2 \widehat{v}_k \mathscr{D}^{-1}\left[\partial \ln(\widehat{\phi}_i z)^{\infty}/\partial x_j\right]_{TP}}{\left(x_j G_{ij}^{\infty,faulty} + x_k G_{ik}^{\infty} + V_c^{faulty}\right)} \tag{A5}$$

which becomes Eq. (28) in §3.2 of the main text. Note that, as the mole fraction of the $j-$ solvent approaches one, the behavior of $G_{ij}^{\infty,faulty}(x_j)$ is described by A1, and thus,

$$\delta_{ji}^{faulty}(x_j \to 1) \to \delta_{ji}(x_j) \tag{A6}$$

which is Eq. (32) in §3.3 of the main text. In other words, despite its faulty nature, $\delta_{ji}^{faulty}(x_j)$ will approach the correct description $\delta_{ji}(x_j)$ at the $x_j = 1$ limit.

To make sense of the above behavior, we analyze in Figs. A1, A2 the composition dependence of the $\left[\partial \Delta_{tr} g_i(x_j)/\partial x_j\right]_{TP}$ according to Eq. (27), as a comparison between the input $\left[\partial \Delta_{tr} g_i(x_j)/\partial x_j\right]_{TP}^{experimental}$ from the regression of the experimental Gibbs free energy of transfer, and the corresponding outcome $\left[\partial \Delta_{tr} g_i(x_j)/\partial x_j\right]_{TP}^{faulty}$. The outstanding features in these pictures are the contrasting signs of the plotted quantities and the corresponding composition slopes, manifested as $\left[\partial \Delta_{tr} g_i(x_j \to small)/\partial x_j\right]_{TP}^{faulty} > 0$ with a negative slope in contrast to the $\left[\partial \Delta_{tr} g_i(x_j \to small)/\partial x_j\right]_{TP}^{experimental} < 0$ with a positive slope.

Moreover, note that from A3 and the definition $\delta_{ji}^{0,faulty} = x_j x_k\left(G_{ij}^{\infty,faulty} - G_{ik}^{\infty}\right)$, we immediately find that the middle root of either $\delta_{ji}^{0,faulty}(x_j) = 0$ or $\delta_{ji}^{faulty}(x_j) = 0$ follows from the condition,

$$\left(x_k\widehat{v}_k - x_j\widehat{v}_j\right) = 0 \tag{A7}$$

leading to solution the numerical or graphical solution of the following expression,

$$x_j = \widehat{v}_k(x_j) \,/\, \left[\widehat{v}_j(x_j) + \widehat{v}_k(x_j)\right] \tag{A8}$$

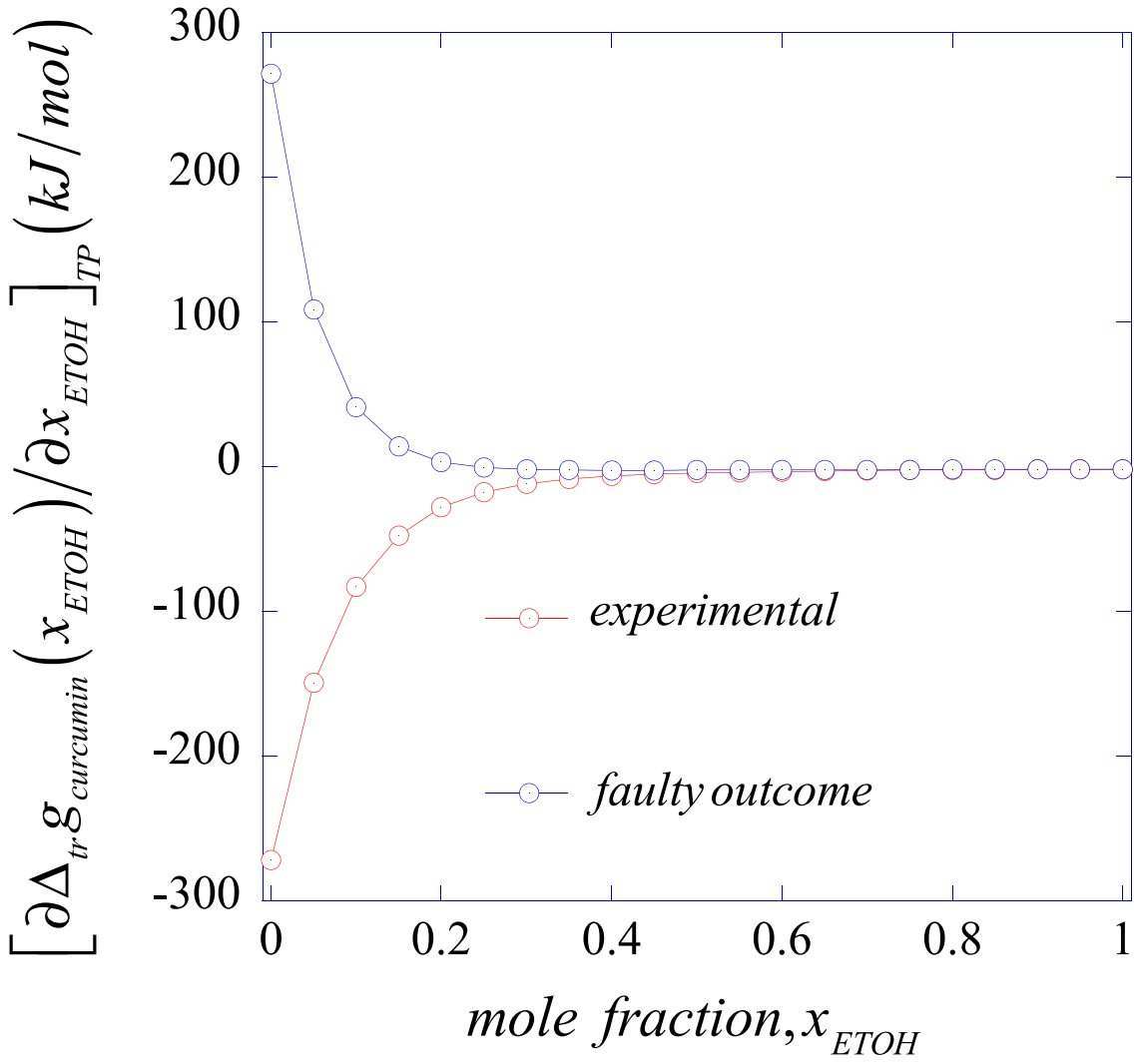

Fig. A1. Comparison between the experimentally available and the faulty outcome of the isothermal-isobaric composition derivative of the transfer Gibbs free energy of curcumin in the curcumin (*i*) in ethanol (*j*) + water (*k*) mixed-solvent at ambient conditions.

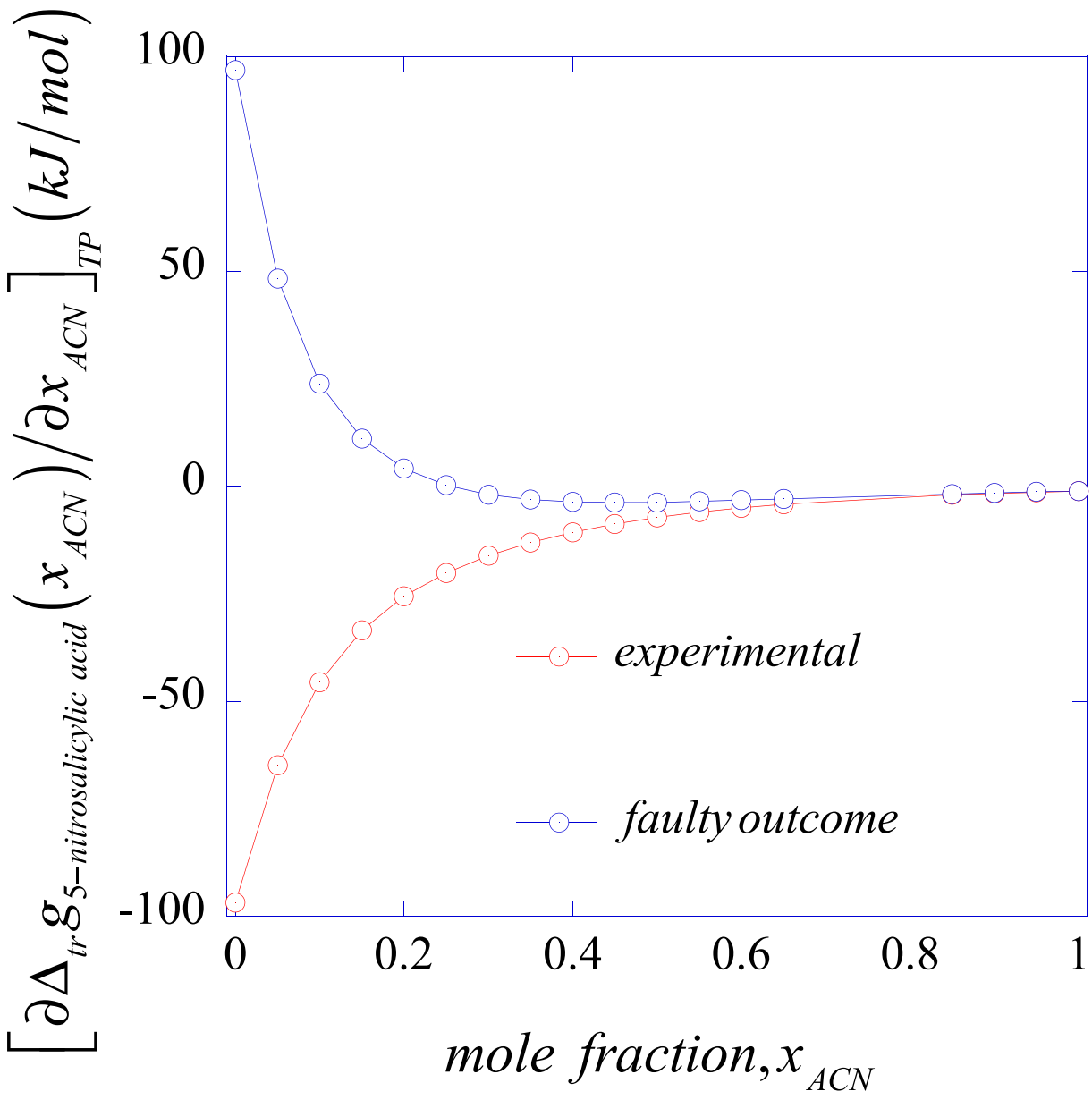

Fig. A2. Comparison between the experimentally available and the faulty outcome of the isothermal-isobaric composition derivative of the transfer Gibbs free energy of 5-nitrosalicylic acid in the 5-nitrosalicylic acid (*i*) in acetonitrile (*j*) + water (*k*) mixed-solvent at ambient conditions.

References

[1] Y. Marcus, The Properties of Solvents, Wiley, 1998.
[2] W.M. Nelson, Green Solvents for Chemistry: Perspectives and Practice, Oxford University Press, 2003.
[3] G. Brunner, Supercritical Fluids as Solvents and Reaction Media, Elsevier B.V., Amsterdam, 2004.
[4] J.G. van Alsten, C.A. Eckert, Effect of entrainers and of solute size and polarity in supercritical-fluid solutions, J. Chem. Eng. Data 38 (1993) 605–610.
[5] A.A. Chialvo, Solute-solute and solute-solvent correlations in dilute near-critical ternary mixtures: mixed solute and entrainer effects, J. Phys. Chem. 97 (1993) 2740–2744.
[6] C.A. Eckert, B.L. Knutson, P.G. Debenedetti, Supercritical fluids as solvents for chemical and materials processing, Nature 383 (1996) 313–318.
[7] D.L. Gurina, E.G. Odintsova, V.A. Golubev, M.L. Antipova, V.E. Petrenko, Features of solvation of phenolic acids in supercritical carbon dioxide modified by methanol and acetone, J. Supercrit. Fluids 124 (2017) 50–56.
[8] T. Momose, A. Kondo, T. Kamiya, H. Yamada, J. Ohara, Y. Kitamura, H. Uchida, Y. Shimogaki, M. Sugiyama, Solubility of bis-(2,2,6,6-tetramethyl-3,5-heptanedionato)copper(II) in mixed supercritical CO_2 and H_2 systems for application in supercritical fluid deposition of Cu, J. Supercrit. Fluids 105 (2015) 193–200.
[9] H. Martin, Kinetic relationships between reactions in the gas phase and in solution, Angew. Chem. 5 (1966) 78–84 (I.E.).
[10] C.A. Eckert, M.R.J. Dack, Molecular thermodynamics of reactions in solution. Solutions and Solubilities, Wiley Intersciences, New York, 1975, pp. 1–28.
[11] J.B.F.N. Engberts, F. Franks, Mixed aqueous solvent effects on kinetics and mechanisms of organic reactions, in: Water: A Comprehensive Treatise, 6, Springer US, Boston, MA, 1979, pp. 139–237. Recent Advances.
[12] C. Cativiela, J.I. Garcia, J. Gil, R.M. Martinez, J.A. Mayoral, L. Salvatella, J. S. Urieta, A.M. Mainar, M.H. Abraham, Solvent effects on Diels-Alder reactions. The use of aqueous mixtures of fluorinated alcohols and the study of reactions of acrylonitrile, J. Chem. Soc. Perkin Trans. 2 (1997) 653–660.
[13] A.A. Chialvo, P.T. Cummings, Y.V. Kalyuzhnyi, Solvation effect on kinetic rate constant of reactions in supercritical solvents, AlChE J. 44 (1998) 667–680.
[14] V.I. Anikeev, A. Yermakova, J. Manion, R. Huie, Kinetics and thermodynamics of 2-propanol dehydration in supercritical water, J. Supercrit. Fluids 32 (2004) 123–135.
[15] B. Subramaniam, R.V. Chaudhari, A.S. Chaudhari, G.R. Akien, Z.Z. Xie, Supercritical fluids and gas-expanded liquids as tunable media for multiphase catalytic reactions, Chem. Eng. Sci. 115 (2014) 3–18.

[16] Z.Z. Xie, W.K. Snavely, A.M. Scurto, B. Subramaniam, Solubilities of CO and H2 in neat and CO2-expanded hydroformylation reaction mixtures containing 1-octene and nonanal up to 353.15 K and 9 MPa, J. Chem. Eng. Data 54 (2009) 1633–1642.

[17] G.R. Akien, M. Poliakoff, A critical look at reactions in class I and II gas-expanded liquids using CO2 and other gases, Green Chem. 11 (2009) 1083–1100.

[18] J.P. Coelho, R.M. Filipe, M.P. Robalo, S. Boyadzhieva, G. St Cholakov, R. P. Stateva, Supercritical CO2 extraction of spent coffee grounds. Influence of co-solvents and characterization of the extracts, J. Supercrit. Fluids 161 (2020) 104825. Art. N°.

[19] Ö. Güçlü-Üstündag, F. Temelli, Solubility behavior of ternary systems of lipids, cosolvents and supercritical carbon dioxide and processing aspects, J. Supercrit. Fluids 36 (2005) 1–15.

[20] J. Rincón, R. Camarillo, L. Rodríguez, V. Ancillo, Fractionation of Used Frying Oil by Supercritical CO2 and Cosolvents, Ind. Eng. Chem. Res. 49 (2010) 2410–2418.

[21] J.T. Rubino, J. Swarbrick, Cosolvents and cosolvency. Encyclopedia of Pharmaceutical Technology, CRC Press, 2006, pp. 806–819.

[22] P.B. Myrdal, S.H. Yalkowsky, J. Swarbrick, Solubilization of drugs in aqueous media. Encyclopedia of Pharmaceutical Technology, CRC Press, 2006, pp. 3311–3333.

[23] Y. Kawashima, M. Imai, H. Takeuchi, H. Yamamoto, K. Kamiya, T. Hino, Improved flowability and compactibility of spherically agglomerated crystals of ascorbic acid for direct tableting designed by spherical crystallization process, Powder Technol. 130 (2003) 283–289.

[24] C. Scherzinger, A. Schwarz, A. Bardow, K. Leonhard, W. Richtering, Cononsolvency of poly-N-isopropyl acrylamide (PNIPAM): microgels versus linear chains and macrogels, Curr Opin Colloid Interface Sci 19 (2014) 84–94.

[25] F. Ren, Y. Zhou, Y. Liu, J. Fu, Q. Jing, G. Ren, A mixed solvent system for preparation of spherically agglomerated crystals of ascorbic acid, Pharm. Dev. Technol. 22 (2016) 818–826.

[26] A.A. Chialvo, E. Matteoli, J.P. O'Connell, P.E. Smith, Solvation phenomena in dilute solutions: formal, experimental evidence, and modeling implications. Fluctuation Theory of Solutions: Applications in Chemistry, Chemical Engineering and Biophysics, CRC Press, Boca Raton, 2013, pp. 191–224.

[27] Y. Marcus, Preferential solvation of ions in mixed-solvents. 4. Comparison of the Kirkwood-Buff and Quasi-Lattice Quasi-chemical approaches, J. Chem. Soc. Faraday Trans. I 85 (1989) 3019–3032.

[28] E. Matteoli, L. Lepori, Kirkwood-Buff integrals and preferential salvation in ternary nonelectrolyte mixtures, J. Chem. Soc. Faraday Trans. 91 (1995) 431–436.

[29] P.E. Smith, Equilibrium dialysis data and the relationships between preferential interaction parameters for biological systems in terms of Kirkwood-Buff integrals, J. Phys. Chem. B 110 (2006) 2862–2868.

[30] P.E. Smith, R.A. Mazo, On the theory of solute solubility in mixed solvents, J. Phys. Chem. B 112 (2008) 7875–7884.

[31] A.A. Chialvo, On the solute-induced structure-making/breaking effect: rigorous links among microscopic behavior, solvation properties, and solution non-ideality, J. Phys. Chem. B 123 (2019) 2930–2947.

[32] A.A. Chialvo, Preferential Solvation Phenomena as Solute-induced Structure-Making/Breaking Processes: linking thermodynamic preferential interaction parameters to fundamental structure making/breaking functions, J. Phys. Chem. B 128 (2024) 5228–5245.

[33] J.G. Kirkwood, F.P. Buff, The Ststistical Mechanical Theory of Solutions. I, J. Chem. Phys. 19 (1951) 774–777.

[34] E. Matteoli, G.A. Mansoori, G.A. Mansoori, Fluctuation theory of mixtures. Advances in Thermodynamics, Taylor and Francis, New York, 1990.

[35] P.E. Smith, E. Matteoli, J.P. O' Connell, Fluctuation theory of solutions: applications in chemistry. Chemical Engineering and Biophysics, CRC Press, Boca Raton, 2013.

[36] A. Ben-Naim, Inversion of Kirkwood-Buff theory of solutions. application to water-ethanol system, J. Chem. Phys. 67 (1977) 4884–4890.

[37] A.A. Chialvo, O.D. Crisalle, Gas solubility and preferential solvation phenomena in mixed-solvents; rigorous relations between microscopic behavior, solvation properties, and solution non-ideality, Fluid Phase Equilib 581 (2024) 114081.

[38] B. Moeser, D. Horinek, The role of the concentration scale in the definition of transfer free energies, Biophys. Chem. 196 (2015) 68–76.

[39] J.P. O'Connell, J.M. Haile, Thermodynamics: Fundamentals for Applications, Cambridge University Press, New York, 2005.

[40] C. Reichardt, T. Welton, Solvents and Solvent Effects in Organic Chemistry, Wiley, 2010.

[41] D.R. Canchi, A.E. Garcia, Cosolvent effects on protein stability, in: M.A. Johnson, T.J. Martinez (Eds.) Annual Review of Physical Chemistry, Vol 64, 2013, pp. 273–293.

[42] N. Nakata, R. Okamoto, T. Sumi, K. Koga, T. Morita, H. Imamura, Molecular mechanism of the common and opposing cosolvent effects of fluorinated alcohol and urea on a coiled coil protein, Protein Sci. 32 (2023) e4763. Art. N°.

[43] G.M. Wilson, Vapor-liquid equilibrium. 11. New expression for excess free energy of mixing, J. Am. Chem. Soc. 86 (1964) 127–130.

[44] D.S. Abrams, J.M. Prausnitz, Statistical thermodynamics of liquids mixtures. New expression for excess gibbs energy of partially miscible, Syst. AlChE J. 21 (1975) 116–128.

[45] H. Renon, J.M. Prausnitz, Local Compositions in thermodynamic excess functions for liquid mixtures, AlChE J. 14 (1968) 135.

[46] A. Fredenslund, R.L. Jones, J.M. Prausnitz, Group contribution estimation of activity coefficients in nonideal liquid mixtures, AlChE J. 21 (1975) 1086–1099.

[47] V. Flemr, Note on excess gibbs energyequations based on local composition concept, Collect. Czechoslov. Chem. Commun. 41 (1976) 3347–3349.

[48] C. McDermott, N. Ashton, Note on the definition of local composition, Fluid Ph. Equilib. 1 (1977) 33–35.

[49] L.L. Lee, T.H. Chung, K.E. Starling, A molecular theory for the thermodynamic behavior of polar mixtures. 1. The statistical-mechanical local-composition mode, Fluid Ph. Equilib. 12 (1983) 105–124.

[50] L.L. Lee, K.E. Starling, The statistical mechanical local composition theory - the balance equations and concentration effects in nonideal mixtures, Fluid Ph. Equilib. 21 (1985) 77–93.

[51] G.A. Mansoori, J.F. Ely, Statistical mechanical Theory of local compositions, Fluid Ph. Equilib. 22 (1985) 253–275.

[52] R.G. Rubio, M.G. Prolongo, U. Cabrerizo, M.D. Pena, J.A.R. Renuncio, Kirkood-Buff integrals in nonelectrolyte solutions. An evaluation of the local composition from experimentl data, Fluid Ph. Equilib. 26 (1986) 1–13.

[53] A. Ben-Naim, Theory of preferential solvation of non-electrolytes, Cell Biophys. 12 (1988) 255–269.

[54] A. Ben-Naim, Preferential solvation in 2-component systems, J. Phys. Chem. 93 (1989) 3809–3813.

[55] A. Ben-Naim, Preferential solvation in 2-component and in 3-component systems, Pure Appl. Chem. 62 (1990) 25–34.

[56] Y. Marcus, Preferential solvation in mixed solvents X. Completely miscible aqueous co-solvent binary mixtures at 298.15 K, Monatsh. Chem. 132 (2001) 1387–1411.

[57] A.A. Chialvo, On the elusive links between solution microstructure, dynamics, and solvation thermodynamics: demystifying the path through a bridge over troubled conjectures and misinterpretations, J. Phys. Chem. B 127 (2023) 10792–10813.

[58] M. Heidari, K. Kremer, R. Potestio, R. Cortes-Huerto, Finite-size integral equations in the theory of liquids and the thermodynamic limit in computer simulations, Mol. Phys. 116 (2018) 3301–3310.

[59] J. Milzetti, D. Nayar, N.F.A. van der Vegt, Convergence of Kirkwood–Buff Integrals of ideal and nonideal aqueous solutions using molecular dynamics simulations, J. Phys. Chem. B 122 (2018) 5515–5526.

[60] Y. Marcus, Solvent Mixtures: Properties and Selective Solvation, Taylor & Francis, 2002.

[61] Y. Marcus, On the preferential solvation of drugs and PAHs in binary solvent mixtures, J. Mol. Liq. 140 (2008) 61–67.

[62] Y. Marcus, Ions in Water and Biophysical Implications: From Chaos to Cosmos, Springer, Dordrecht, Netherlands, 2012.

[63] Y. Marcus, Ions in Solution and Their Solvation, John Wiley and Sons, Hoboken, N.J., 2015.

[64] Y. Marcus, Preferential solvation in mixed-solvents. 5. Binaary Mixtures of Water and Organic Solvents Journal of the Chemical Society-Faraday Transactions, 86 (1990) 2215–2224.

[65] Y.Z. Shen, A. Farajtabar, J. Xu, J.L. Wang, Y.Y. Xia, H.K. Zhao, R.J. Xu, Thermodynamic solubility modeling, solvent effect and preferential solvation of curcumin in aqueous co-solvent mixtures of ethanol, *n*-propanol, isopropanol and propylene glycol, J. Chem. Thermodyn. 131 (2019) 410–419.

[66] Q.R. Guo, W.Z. Shi, H.K. Zhao, W.X. Li, G. Han, A. Farajtabar, Solubility, solvent effect, preferential solvation and DFT computations of 5-nitrosalicylic acid in several aqueous blends, J. Chem. Thermodyn. 177 (2023) 106936. Art. N°.

[67] A.A. Chialvo, O.D. Crisalle, Solute-induced perturbation of the solvent microstructure in aqueous electrolyte solutions: some uses and misuses of structure making/breaking criteria, Liquids 2 (2022) 106–130.

[68] A.A. Chialvo, Molecular-based description of the osmotic second virial coefficients of electrolytes: rigorous formal links to solute−solvent interaction asymmetry, virial expansion paths, and experimental evidence, J. Phys. Chem. B 126 (2022) 4339–4353.

[69] E.A. Moelwyn-Hughes, P.L. Thorpe, R.G.W. Norrish, The physical and thermodynamic properties of some associated solutions II. Heat capacities and compressibilities, in: Proceedings of the Royal Society of London. Series A. Mathematical and Physical Sciences 278, 1964, pp. 574–587.

[70] R.W. Missen, Use of term "excess function", Ind. Eng. Chem. Fundam. 8 (1969) 81–84.

[71] A.R. Tagliaferro, J.R. Davis, S. Truchon, N. Van Hamont, Effects of dehydroepiandrosterone acetate on metabolism, body weight and composition of male and female rats, J. Nutr. 116 (1986) 1977–1983.

[72] J. Sonka, Dehydroepiandrosterone. Metabolic effects, Acta Univ. Carol. Med. Monogr. 71 (1976) 1–137, 146-171.

[73] C. Cheng, Y. Cong, L. Meng, J. wang, G. Yao, H. Zhao, Solubility measurement and thermodynamic functions of dehydroepiandrosterone acetate in different solvents at evaluated temperatures, J. Chem. Thermodyn. 97 (2016) 158–166.

[74] C. Cheng, Y. Cong, C.B. Du, J. Wang, G.B. Yao, H.K. Zhao, Solubility determination and thermodynamic models for dehydroepiandrosterone acetate in mixed solvents of (ethyl acetate plus methanol), (ethyl acetate plus ethanol) and (ethyl acetate plus isopropanol), J. Chem. Thermodyn. 101 (2016) 372–379.

[75] X.B. Li, Y. Liu, J. Chen, G.Q. Chen, H.K. Zhao, Preferential solvation of dehydroepiandrosterone acetate in (co-solvent plus ethyl acetate) mixtures according to the inverse Kirkwood-Buff integrals method, J. Chem. Thermodyn. 111 (2017) 149–156.

[76] M.A. Ruidiaz, E.F. Vargas, F. Martinez, Study of some volumetric properties of the pharmaceutical model solvent system ethanol + ethyl acetate at several temperatures, Latin Am. J. Pharm. 29 (2010) 306–312.

[77] S.L. Oswal, S.S.R. Putta, Excess molar volumes of binary mixtures of alkanols with ethyl acetate from 298.15 to 323.15 K, Thermochim. Acta 373 (2001) 141–152.

[78] P. Murti, M. Van Winkle, Vapor-liquid equilibria for binary systems of methanol, ethyl alcohol, 1-propanol, and 2-propanol with ethyl acetate and 1-propanol-water, Ind. Eng. Chem. Chem. Eng. Data Ser. 3 (1958) 72–81.
[79] G.A. Rodríguez, D.R. Delgado, F. Martínez, Preferential solvation of indomethacin and naproxen in ethyl acetate plus ethanol mixtures according to the IKBI method, Phys. Chem. Liq. 52 (2014) 533–545.
[80] D.M. Cristancho, F. Martínez, Solubility and preferential solvation of meloxicam in ethyl acetate plus ethanol mixtures at several temperatures, J. Mol. Liq. 200 (2014) 122–128.
[81] D.M. Cristancho, A. Jouyban, F. Martínez, Solubility, solution thermodynamics, and preferential solvation of piroxicam in ethyl acetate plus ethanol mixtures, J. Mol. Liq. 221 (2016) 72–81.
[82] Z. Guoquan, Study of solute-solvent intermolecular interactions and preferential solvation for mevastatin dissolution in pure and mixed binary solvents, J. Chem. Thermodyn. 175 (2022) 106884. Art. N°.
[83] C.B. Du, Y. Cong, M. Wang, Z.Y. Jiang, M.L. Wang, Preferential solvation and solute-solvent interactions of posaconazole in mixtures of (ethyl acetate plus ethanol/isopropanol) at several temperatures, J. Chem. Thermodyn. 165 (2022).
[84] R.M. Mazo, Statistical Mechanical Theory of Solutions, J. Chem. Phys. 29 (1958) 1122–1128.
[85] E. Ruckenstein, I. Shulgin, Solubility of drugs in aqueous solutions - Part 2: binary nonideal mixed solvent, Int. J. Pharm. 260 (2003) 283–291.
[86] E. Ruckenstein, I. Shulgin, Solubility of hydrophobic organic pollutants in binary and multicomponent aqueous solvents, Environ. Sci. Technol. 39 (2005) 1623–1631.
[87] Mayo Clinic, Drugs & supplements 2024, https://www.mayoclinic.org/drugs-supplements.
[88] C.F. Anderson, E.S. Courtenay, M.T. Record, Thermodynamic expressions relating different types of preferential interaction coefficients in solutions containing two solute components, J. Phys. Chem. B 106 (2002) 418–433.
[89] C.F. Anderson, D.J. Felitsky, J. Hong, M.T. Record, Generalized derivation of an exact relationship linking different coefficients that characterize thermodynamic effects of preferential interactions, Biophys. Chem. 101 (2002) 497–511.
[90] X. Zhao, A. Farajtabar, G. Han, H.H. Zhao, Griseofulvin dissolved in binary aqueous co-solvent mixtures of *N,N*-dimethylformamide, methanol, ethanol, acetonitrile and *N*-methylpyrrolidone: solubility determination and thermodynamic studies, J. Chem. Thermodyn. 151 (2020) 106250. Art. N°.
[91] S. Alshehri, F. Shakeel, P. Alam, A. Jouyban, F. Martinez, Solubility of 6-phenyl-4,5-dihydropyridazin-3(2*H*)-one in aqueous mixtures of Transcutol and PEG 400 revisited: correlation and preferential solvation, J. Mol. Liq. 344 (2021) 117728. Art N°.
[92] A. Noubigh, M. Abderrabba, Preferential solvation of 5,7-dihydroxyflavone (chrysin) in aqueous co-solvent mixtures of methanol and ethanol, Phys. Chem. Liq. 60 (2022) 931–942.
[93] Q. Gao, A. Farajtabar, Glyburide in a series co-solvent solutions: solubility and modeling, solvation and quantum chemistry research, J. Chem. Thermodyn. 189 (2024).
[94] A. Jouyban, S. Nozohouri, F. Martinez, Solubility of celecoxib in {2-propanol (1) + water (2)} mixtures at various temperatures: experimental data and thermodynamic analysis, J. Mol. Liq. 254 (2018) 1–7.
[95] X.B. Li, Y.T. He, Y.Y. Xu, X.T. Zhang, M. Zheng, H.K. Zhao, 5-Nitrosalicylaldehyde in aqueous co-solvent mixtures of methanol, ethanol, isopropanol and acetonitrile: solubility determination, solvent effect and preferential solvation analysis, J. Chem. Thermodyn. 142 (2020) 106014. Art No.
[96] Q.R. Guo, W.Z. Shi, H.K. Zhao, W.X. Li, A. Farajtabar, Equilibrium solubility, non-covalent interactions and solvation thermodynamics of thiamphenicol in aqueous cosolvents of n-propanol/acetone/acetonitrile, J. Chem. Thermodyn. 178 (2023) 106972. Art #.
[97] X. Li, M. Ma, J. Chen, G. Chen, H. Zhao, Preferential solvation of boscalid in ethanol/isopropanol + ethyl acetate mixtures from the inverse Kirkwood–Buff integrals method, J. Solution Chem. 46 (2017) 2050–2065.
[98] Y.Q. Zhu, C. Cheng, H.K. Zhao, Solubility and preferential solvation of carbazochrome in solvent mixtures of *N,N*-dimethylformamide plus methanol/ethanol/*n*-propanol and dimethyl sulfoxide plus water, J. Chem. Eng. Data 63 (2018) 822–831.
[99] M. Zheng, J. Chen, R.J. Xu, G.Q. Chen, Y. Cong, H.K. Zhao, Solubility and preferential solvation of 3-nitrobenzonitrile in binary solvent mixtures of ethyl acetate plus (methanol, ethanol, *n*-propanol, and isopropyl alcohol), J. Chem. Eng. Data 63 (2018) 2290–2298.
[100] A. Romdhani, I.P. Osorio, F. Martínez, A. Jouyban, W.E. Acree, Further calculations on the solubility of *trans*-resveratrol in (Transcutol® plus water) mixtures, J. Mol. Liq. 330 (2021) 115645. Art. N°.
[101] I.P. Osorio, F. Martínez, M.A. Peña, A. Jouyban, W.E. Acree, Solubility of sulphadiazine in some {Carbitol® (1) + water (2)} mixtures: determination, correlation, and preferential solvation, Phys. Chem. Liq. 59 (2021) 890–906.
[102] A. Noubigh, L. Ben Tahar, A. Eladeb, Solubility modeling and preferential solvation of benzamide in some pure and binary solvent mixtures at different temperatures, J. Chem. Eng. Data 68 (2023) 1018–1030.
[103] I.R. Krichevskii, Thermodynamics of an infinitely dilute solution in mixed solvents. I. The Henry's coefficient in a mixed solvent behaving as an ideal solvent, Zhournal Fiz. Khimii 9 (1937) 41–47. English translation by Dr. Olesya Bondarenko.
[104] K.E. Newman, Application of Kirkwood-Buff theory to enthalpies of transfer and expansivities of solutes, Bin. Solvent Mix. J. Chem. Soc. Faraday Trans. I 84 (1988) 3885–3890.